VOLUME 112, NUMBER 22
OCTOBER 24, 1990

JOURNAL
OF THE
AMERICAN
CHEMICAL
SOCIETY

A Time-Resolved IR Study of the Gas-Phase Reactions of 1,3- and 1,4-Pentadiene with $Cr(CO)_4$

Steven J. Gravelle and Eric Weitz*

Contribution from the Department of Chemistry, Northwestern University, Evanston, Illinois 60208-3113. *Received December 15, 1989. Revised Manuscript Received June 11, 1990*

Abstract: The reactions of 1,3- and 1,4-pentadiene (PD) with the coordinatively unsaturated species $Cr(CO)_4$ were probed with time-resolved infrared spectroscopy in an effort to compare the reactivities of conjugated and nonconjugated dienes toward metal carbonyls. Both spectroscopic and kinetic evidence that indicates the addition of pentadiene to $Cr(CO)_4$ follows a branched reaction mechanism. Formation of the initial product, highly excited $[(\eta^4\text{-PD})Cr(CO)_4]^*$, occurs with rate constants that are near gas kinetic: $(6 \pm 2) \times 10^{14}$ cm^3 mol^{-1} s^{-1} for 1,3-pentadiene and $(4 \pm 2) \times 10^{14}$ cm^3 mol^{-1} s^{-1} for 1,4-pentadiene. This excited complex can rearrange via bond scission to form $(\eta^2\text{-PD})Cr(CO)_4$ or, at high buffer gas pressures, collisionally relax to form $(\eta^4\text{-PD})Cr(CO)_4$. In the 1,3-pentadiene system, $(\eta^2\text{-1,3-PD})Cr(CO)_4$ forms stable $(\eta^4\text{-1,3-PD})Cr(CO)_4$ in an unactivated but slow $[(2.2 \pm 0.9) \times 10^3$ s$^{-1}]$ rearrangement. In contrast, $(\eta^2\text{-1,4-PD})Cr(CO)_4$ is unreactive on a millisecond time scale, while the $(\eta^4\text{-1,4-PD})Cr(CO)_4$ formed by collisional relaxation of the initial complex rearranges to a more stable isomeric species. It is likely that this more stable isomer is $(\eta^{2:CH}\text{-1,4-PD})Cr(CO)_4$, where $\eta^{2:CH}$ represents an agostic Cr–H–C bond. This latter reaction is activated $[(11.4 \pm 0.4)$ kcal/mol] and has a first-order rate constant of $(4.5 \pm 1.3) \times 10^4$ s^{-1} at room temperature. The factors that lead to the differences in the reaction mechanism for 1,3- versus 1,4-pentadiene with $Cr(CO)_4$ are discussed.

I. Introduction

The photochemistry of metal carbonyls is an actively studied field due to the wide variety of synthetic and catalytic precursors that can be generated by photolysis of these species. Important catalytic processes induced by these species, which typically contain a metal carbonyl fragment complexed to an olefin, include hydrosilation,[1] hydrogenation,[2-4] and olefin isomerization.[5-10] Two particularly interesting coordinatively unsaturated metal carbonyls are the bis-unsaturated species $Fe(CO)_3$ (d^8 metal center) and $Cr(CO)_4$ (d^6 metal center). Although both require 4 electrons from a donating ligand(s) to form a stable 18-electron species, their reactive behavior can be very different.

In the iron system, Fleckner, Grevels, and Hess[9] have observed that bis-olefin complexes such as $(cyclooctene)_2Fe(CO)_3$ can catalytically isomerize 1-pentene but that this catalytic behavior is halted by the addition of a 1,3-diene (a conjugated diene), which forms the stable $(\eta^4\text{-1,3-diene})Fe(CO)_3$ complex. They have also observed the isomerization of nonconjugated 1,4-dienes to con-

(1) Hill, R. H.; Wrighton, M. S. *Organometallics* **1987**, *6*, 632. Hill, R. H.; Wrighton, M. S. *Organometallics* **1987**, *4*, 413.
(2) (a) Miller, M. E.; Grant, E. R. *J. Am. Chem. Soc.* **1984**, *106*, 4635. (b) Miller, M. E.; Grant, E. R. *J. Am. Chem. Soc.* **1987**, *109*, 7951.
(3) (a) Schroeder, M. A.; Wrighton, M. S. *J. Am. Chem. Soc.* **1976**, *98*, 551. (b) Schroeder, M. A.; Wrighton, M. S. *J. Organomet. Chem.* **1974**, *74*, C29.
(4) Frankel, E. N.; Selke, E.; Glass, C. A. *J. Am. Chem. Soc.* **1968**, *90*, 2446.
(5) Aumann, R. *J. Am. Chem. Soc.* **1974**, *96*, 2631.
(6) Casey, C. P.; Cyr, C. R. *J. Am. Chem. Soc.* **1973**, *95*, 2248.
(7) Tumas, W.; Gitlin, B.; Rosan, A. M.; Yardley, J. T. *J. Am. Chem. Soc.* **1982**, *104*, 55.
(8) Wuu, Y.-M.; Bentsen, J. G.; Brinkley, C. G.; Wrighton, M. S. *Inorg. Chem.* **1987**, *26*, 530.
(9) Fleckner, M.; Grevels, F.-W.; Hess, D. *J. Am. Chem. Soc.* **1984**, *106*, 2027.
(10) Leigh, G. J.; Fischer, E. O. *J. Organomet. Chem.* **1965**, *4*, 461.

0002-7863/90/1512-7839$02.50/0

jugated 1,3-dienes in the presence of $Fe(CO)_3$, again forming (η^4-1,3-diene)$Fe(CO)_3$.

Examples of catalytic isomerization of olefins by $Cr(CO)_4$ include conversion of 1-butene to 2-butene[7] and 1,5-cyclooctadiene to *o*-xylene.[10] However, in contrast to the iron system, $Cr(CO)_4$ often forms stable complexes more readily with nonconjugated than conjugated dienes.[11] For example, Dixon et al.[12] have observed the thermal replacement of conjugated ligands in (1,3-butadiene)$Cr(CO)_4$ and (2,4-hexadiene)$Cr(CO)_4$ by nonconjugated cyclooctadiene and norbornadiene.

Using molecular orbital theory, Elian and Hoffmann[11] predicted that $Cr(CO)_4$ should bond more readily with dienes containing nonconjugated ethylene groups, while $Fe(CO)_3$ should bond more readily with conjugated π systems. Two exceptions to these trends have been observed for $Cr(CO)_4$. First, although $Cr(CO)_4$ forms stable (η^4-diene)$Cr(CO)_4$ complexes with the large nonconjugated ligands mentioned above, $Cr(CO)_4$ seems to prefer bonding with the conjugated form of smaller diene ligands such as pentadiene and hexadiene.[13] Second, although Elian and Hoffmann's calculations imply that *cis*-(olefin)$_2Cr(CO)_4$ complexes should be stable, the only complex of that type is $(C_2H_4)_2Cr(CO)_4$,[14,15] although both cis and trans structures of (olefin)$_2M(CO)_4$ have been observed for olefins larger than C_2H_4 when M = Mo, W.[16-18] Even $(C_2H_4)_2Cr(CO)_4$ is not that stable. The decay rate for $(C_2H_4)_2Cr(CO)_4$ in the gas phase is 6×10^4 s^{-1},[19] several orders of magnitude larger than the solution-phase value for (η^4-butadiene)$Cr(CO)_4$ (2×10^{-3} s^{-1}),[12] its conjugated analogue.

In the studies discussed above, reaction mechanisms have been inferred from observing the saturated products rather than the unsaturated intermediates. In other systems, direct monitoring of unsaturated intermediates with time-resolved IR (TRIR) spectroscopy in the gas phase has proven to be a useful tool for elucidating the reactivity of metal carbonyls free from solvent effects.[20] It is clear that gas-phase studies are necessary to probe the reactivity of naked metal carbonyl species with desired ligands. In solution, the putative "coordinatively unsaturated" metal carbonyl will generally be complexed with solvent. Thus, the rate-limiting step in ligand addition may not be dominated by the interaction of the coordinatively unsaturated species with incoming ligand but rather by dissociative loss of solvent. If this occurs, details of ligand-specific interactions with the coordinatively unsaturated species will be lost.

Several studies have also been undertaken to understand the wavelength dependence of metal carbonyl photofragmentation processes and the IR spectra of the resulting transients.[21] Other studies have shown that the rate of reaction of metal carbonyl photofragments with small molecules often approaches the gas-kinetic limit[21,22] and that the products of photofragment recombination with CO are usually formed with significant internal excitation.[23] However, this technique has rarely been used to completely map out a reaction mechanism.

In this study, TRIR spectroscopy is used to monitor the intermediates and products formed from the addition of conjugated and nonconjugated dienes to $Cr(CO)_4$ in the gas phase. By contrasting the reactivities of these two types of dienes toward $Cr(CO)_4$, controlling factors in the complexation of olefins with metal carbonyls may be discerned. Finally, a companion study has been undertaken[24] that compares the reactivity of $Fe(CO)_3$ with conjugated and nonconjugated dienes in order to observe the effect of the metal center (Fe vs. Cr) on the reactivity of bis-unsaturated metal carbonyls with diene ligands.

II. Experimental Section

The apparatus used to photolyze $Cr(CO)_6$ in the gas phase has been described previously.[21] Briefly, sample gases containing $Cr(CO)_6$, pentadiene, and Ar buffer were introduced into a flow cell and photolyzed by a pulsed UV excimer laser (Questek 2000 series operated at 248 nm with KrF). The fluence of the excimer laser was typically between 3 and 5 mJ/cm^2, which photolyzed no more than ~20% of the $Cr(CO)_6$ parent. Growth and decay of the transient species formed by the UV photolysis of $Cr(CO)_6$ and the subsequent reaction of $Cr(CO)_4$ with pentadiene were detected by monitoring the change in intensity of a CO laser which was double-passed through the gas-flow cell and tuned over the carbonyl stretching region, 2030–1880 cm^{-1}. The change in intensity of the CO laser was monitored by an InSb detector (Santa Barbara Research Corp.) whose signals were amplified (Perry, 100×) and sent to a LeCroy 9400 digital oscilloscope for digitization and averaging. The measured risetime of the acquisition equipment in these experiments is ~70 ns.

Transient IR absorption signals were acquired during the first 100 ns to 2 ms following photolysis of $Cr(CO)_6$. The digital oscilloscope was triggered with a photodiode placed in the UV beam path. The background intensity of the CO laser (I_0) was recorded prior to photolysis by measuring the amplitude of the chopped CO laser beam. Each signal was recorded along with its I_0 value on an IBM-AT microcomputer and later plotted in units of percent transmittance or absorbance. Spectra were generated by connecting points at common delay times from signals taken at different frequencies. Signals at selected frequencies were analyzed with a multiexponential signal analysis routine developed by Provencher.[25] Long-lived products were monitored by using a single scan of a Mattson "Polaris" FTIR spectrometer run at 1-cm^{-1} resolution.

Two different types of gas-flow cells were available for each experiment. The flow cell used for generating time-resolved spectra has, in addition to a central sample gas inlet, two Ar purge gas inlets near the ends of the cell that allow Ar to flow over the windows of the cell to prevent buildup of polynuclear species on the windows. The flow cell used in the studies involving detailed kinetics contains only a single central sample gas inlet and no Ar purge gas inlets. This simpler design allows more accurate determination of pressure-dependent rate constants by avoiding uncertainties in the flow rates of the sample gas due to the presence of the purge gas. However, this cell requires more frequent cleaning of the windows.

The flow rate of each component in the sample gas was set with Tylan mass flow controllers so that the sample gas, which typically consisted of 5–20 mTorr of $Cr(CO)_6$, 0–2 Torr of 1,3- or 1,4-pentadiene, and enough Ar buffer and window purge gas (when used) to bring the total pressure to at least 6 Torr, was replenished between each UV laser pulse. $Cr(CO)_6$ (99% purity) was obtained from Aldrich and sublimed in situ. *trans*-1,3-Pentadiene (98% purity) and 1,4-pentadiene (99% purity) were obtained from Aldrich and Wiley Organics. These dienes were subjected to several freeze–pump–thaw cycles before use. Ar (99.99+% purity) and CO (99.99% purity) were obtained from Matheson and used without further purification.

Since 248-nm radiation is weakly absorbed by pentadienes, these species were separately irradiated at high pressure (150 Torr) for 15 000 laser shots. There was no significant difference between IR spectra of the samples taken before and after irradiation, indicating that no appreciable loss of material or isomerization reactions take place in neat pentadiene samples as a result of the absorption of energy at this wavelength. Additionally, the absorption coefficients of 1,3- and 1,4-pentadiene differ by a factor of over 200 at 248 nm (204 vs 0.89 M^{-1} cm^{-1}), while the short time reactive behavior of both species with $Cr(CO)_4$ was found to be very similar. These observations indicate that the small

(11) Elian, M.; Hoffmann, R. *Inorg. Chem.* **1975**, *14*, 1058.
(12) Dixon, D. T.; Burkinshaw, P. M.; Howel, J. S. *J. Chem. Soc., Dalton Trans.* **1980**, 2237.
(13) Without commenting on the trends observed in ref 11, Kreiter and co-workers have generated a number of (diene)$Cr(CO)_4$ complexes with small, conjugated dienes. See: Kreiter, C. G. *Adv. Organomet. Chem.* **1986**, *26*, 297 and references therein.
(14) Weiller, B. H.; Grant, E. R. *J. Phys. Chem.* **1988**, *92*, 1458.
(15) Gregory, M. F.; Jackson, S. A.; Poliakoff, M.; Turner, J. J. *J. Chem. Soc., Chem. Commun.* **1986**, 1175.
(16) Stolz, I. W.; Robson, G. R.; Sheline, R. K. *Inorg. Chem.* **1963**, *2*, 1264.
(17) (a) Grevels, F.-W.; Skibbe, V. *J. Chem. Soc., Chem. Commun.* **1984**, 681. (b) Grevels, F.-W.; Jacke, J.; Ozkar, S. *J. Am. Chem. Soc.* **1987**, *109*, 7536. (c) Grevels, F.-W.; Jacke, J.; Klotzbucher, W. E.; Ozkar, S.; Skibbe, V. *Pure Appl. Chem.* **1988**, *60*, 1017.
(18) Pope, K. R.; Wrighton, M. S. *Inorg. Chem.* **1985**, *24*, 2792.
(19) Weiller, B. H.; Grant, E. R. *J. Am. Chem. Soc.* **1987**, *109*, 1051. Weiller, B. H.; Miller, M. E.; Grant, E. R. *J. Am. Chem. Soc.* **1987**, *109*, 352.
(20) Poliakoff, M.; Weitz, E. *Adv. Organomet. Chem.* **1986**, *25*, 277.
(21) (a) Seder, T. A.; Ouderkirk, A. J.; Weitz, E. *J. Chem. Phys.* **1986**, *85*, 1977. (b) Seder, T. A.; Church, S. P.; Weitz, E. *J. Am. Chem. Soc.* **1986**, *108*, 4721. (c) Seder, T. A.; Church, S. P.; Weitz, E. *J. Am. Chem. Soc.* **1986**, *108*, 7518.
(22) Fletcher, T. R.; Rosenfeld, R. N. *J. Am. Chem. Soc.* **1986**, *108*, 1686.
(23) Ishikawa, Y.; Hackett, P. A.; Rayner, D. M. *Chem. Phys. Lett.* **1988**, *145*, 429.
(24) Gravelle, S. J.; van de Burgt, L. J.; Weitz, E. Submitted for publication.
(25) Provencher, S. W. *Biophys. J.* **1976**, *16*, 27. Provencher, S. W. *J. Chem. Phys.* **1976**, *64*, 2772.

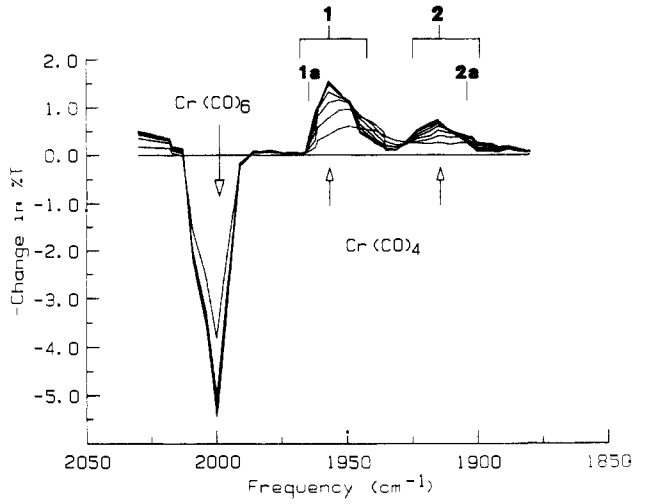

Figure 1. Time-resolved spectrum resulting from the KrF excimer laser (248 nm) photolysis of 7 mTorr of $Cr(CO)_6$ in 7.2 Torr of Ar. The y axis represents the percent change in transmission and the x axis is in wavenumbers. A positive-going band represents the growth of a photoproduct, while a negative-going band indicates depletion of a species. The spectrum covers a total time range of 0.8 μs, with each successive trace incremented by 0.1 μs. The direction of growth or decay at peak absorptions is indicated by arrows. See Table I for a summary of IR band assignments.

absorption of radiation by the pentadienes plays no role in the observed reactions.

Unless otherwise stated, all experiments were conducted at 298 K. For those studies where the sample gas temperature was varied, water heated to between 298 and 336 K flowed through a jacket surrounding the photolysis cell. Thermal equilibration between the sample gas and the hot water jacket was verified by monitoring a thermocouple placed inside the cell.

III. Results and Discussion

To elucidate the mechanisms governing the reactions of 1,3- and 1,4-pentadiene with $Cr(CO)_4$, the spectra and kinetic behavior of the reactants, intermediates, and products were observed in the gas phase. In the following discussion, tentative assignments of the species involved in a reaction mechanism are provided by comparing the band positions in the time-resolved spectra with the known spectra of similar compounds. A general outline of the mechanism is then formulated by monitoring the temporal behavior of these species. Finally, a detailed kinetic analysis of the mechanism is performed by monitoring these species under various conditions of pressure and temperature. To investigate potential reactions competing with the addition of pentadiene to $Cr(CO)_4$, it was first necessary to carefully monitor the reaction kinetics of $Cr(CO)_4$ with $Cr(CO)_6$.

A. $Cr(CO)_6$ Photolysis. $Cr(CO)_4$, the dominant photoproduct following 248-nm photolysis of $Cr(CO)_6$ in the gas phase,[21b,7] adopts a low-symmetry C_{2v} structure in both the gas and condensed phases.[26] This low symmetry implies that the IR spectrum of $Cr(CO)_4$ contains four allowed CO stretching mode absorptions and that the attachment of two olefins to this unsaturated fragment should form a *cis*-(olefin)$_2$Cr(CO)$_4$ structure if the C_{2v} symmetry of the original $Cr(CO)_4$ fragment is retained. This latter prediction is borne out by experiment; *cis*-$(C_2H_4)_2Cr(CO)_4$ is formed in the gas phase following pulsed UV photolysis of $Cr(CO)_6$ in the presence of C_2H_4,[14,27] while formation of the trans isomer in solution phase requires continuous UV irradiation of $Cr(CO)_6$ with C_2H_4.[17b,c] In both systems, the addition of C_2H_4 to $Cr(CO)_4$ most likely results in the initial formation of *cis*-$(C_2H_4)_2Cr(CO)_4$, which, in the solution phase, is photoisomerized by prolonged irradiation to the more stable trans structure.[17c]

The transient IR spectrum resulting from the 248-nm KrF laser photolysis of 7 mTorr of $Cr(CO)_6$ in 7.2 Torr of Ar is shown in Figure 1. Seder et al.[21b] have assigned the negative going feature (due to depletion of parent) at 2000 cm^{-1} to the T_{1u} mode of $Cr(CO)_6$ and the absorptions centered at 1957 cm^{-1} and 1920 cm^{-1} to three of the CO stretching modes of the $Cr(CO)_4$ photoproduct. The fourth $Cr(CO)_4$ carbonyl absorption, expected to absorb around 2070 cm^{-1} is out of the range of operation of the CO laser.

Scheme I

$$Cr(CO)_6 \xrightarrow[h\nu]{248\ nm} [Cr(CO)_4]^* + 2CO \quad (1a)$$

$$[Cr(CO)_4]^* + M \xrightarrow{k_1} Cr(CO)_4 + M \quad (1b)$$

$$Cr(CO)_4 + Cr(CO)_6 \xrightarrow{k_2} Cr_2(CO)_{10} \quad (2)$$

At frequencies above 2010 cm^{-1}, absorptions were observed due to internally excited CO (CO*), which increase significantly in amplitude above ~2030 cm^{-1} and obscure other absorptions that might occur in this region. Because of these interfering CO* absorptions, the spectra displayed in this paper only cover the region below 2030 cm^{-1}. Seder et al.[21b] also report the formation of a small amount of $Cr(CO)_5$ following 248-nm photolysis of $Cr(CO)_6$. Since this species is formed in very small quantities (as evidenced by its negligible absorption at 1980 cm^{-1} in Figure 1), it plays an insignificant role in the reaction mechanism under study. Further, since the positions of (η^2-pentadiene)$Cr(CO)_5$ absorptions are known and these are stable complexes (vide infra), formation of small amounts of these compounds does not interfere with the study of diene complexes of $Cr(CO)_4$.

While the apparent rate of primary photolytic depletion of $Cr(CO)_6$ in Figure 1 is limited by the system risetime of 70 ns, it can be seen that the rise rate of $Cr(CO)_4$, absorption bands **1** and **2** in Figure 1, is significantly slower. Additionally, absorption bands **1** and **2** narrow and shift to higher frequency during the first microsecond following photolysis. This narrowing and shifting of the IR spectrum is due to the relaxation of the initially formed $[Cr(CO)_4]^*$, which is internally excited[21b] and which relaxes on the time scale depicted in Figure 1.

The relaxation of excited $[Cr(CO)_4]^*$ to $Cr(CO)_4$ was monitored by probing selected frequencies in the spectrum in Figure 1. Since the initially formed $[Cr(CO)_4]^*$ absorbs at lower frequencies than relaxed $Cr(CO)_4$, $[Cr(CO)_4]^*$ was probed at 1906 cm^{-1} (**2a**), on the low-frequency edge of band **2** in Figure 1, and the formation of relaxed $Cr(CO)_4$ was monitored at 1965 cm^{-1} (**1a**), on the high-frequency edge of band **1** in the same figure. The fall rate of $[Cr(CO)_4]^*$ at **2a** equals the formation rate of $Cr(CO)_4$ at **1a**. The rate of this process is $(2.8 \pm 0.2) \times 10^6$ s^{-1} under the conditions of the experiment (5–20 mTorr $Cr(CO)_6$ with sufficient Ar buffer gas to maintain a constant total cell pressure of 7.2 Torr).

Another characteristic of this system, seen on a longer time scale than displayed in Figure 1, is the secondary depletion of $Cr(CO)_6$ and $Cr(CO)_4$ caused by the reaction of these two species to form a polynuclear species, presumably $Cr_2(CO)_{10}$.[22] The reaction of $Cr(CO)_4$ with $Cr(CO)_6$ was monitored by following the rate of $Cr(CO)_4$ depletion at 1965 cm^{-1} (**1a** in Figure 1) and the secondary decay rate of $Cr(CO)_6$ (the loss of $Cr(CO)_6$ subsequent to photolysis) at 2000 cm^{-1} while varying the $Cr(CO)_6$ pressure from 5 to 20 mTorr. The rates of loss of $Cr(CO)_4$ and $Cr(CO)_6$ are equal and increase linearly with the $Cr(CO)_6$ pressure, giving a bimolecular rate constant of $(3.7 \pm 0.4) \times 10^{14}$ cm^3 mol^{-1} s^{-1}, which agrees well with previous results by Fletcher and Rosenfeld.[22] The error limits reported for this and other reaction rates indicate the 95% confidence levels.

None of the rates for reaction of $Cr(CO)_4$ show a dependence on UV excimer energy, indicating that the reaction of $Cr(CO)_4$ with itself is an insignificant process under these conditions, and that, as outlined in Scheme I, the primary channel for loss of $Cr(CO)_4$ under these conditions is reaction with $Cr(CO)_6$. (In this scheme, M refers to the buffer gas.)

It can be concluded that $Cr(CO)_4$ is formed in a range of internally (vibrationally and rotationally) excited states following 248-nm photolysis of $Cr(CO)_6$ and that internally relaxed $Cr(CO)_4$

(26) Perutz, R. N.; Turner, J. J. *J. Am. Chem. Soc.* **1975**, *97*, 4800.
(27) Weiller, B. H.; Grant, E. R. *J. Am. Chem. Soc.* **1987**, *109*, 1252.

Table I. IR Absorptions of Related Compounds Containing the $Cr(CO)_4$ Fragment[a]

compd (conditions)	IR freq, cm^{-1} (rel amplitudes)					ref
1. $Cr(CO)_4$ (gas, 298 K)			1957 (1.0)		1920 (0.46)	21b
$Cr(CO)_4$ (CH_4 matrix, 20 K)	2051	1935	(unassigned region)	1929	1888	26
2. (η^2-C_2H_4)$W(CO)_4$	2047		(unassigned region)		1883	18
(η^2-C_3H_6)$W(CO)_4$	2044		(unassigned region)		1885	18
(η^2-C_3H_6)$_2W(CO)_4$	2039		(unassigned region)		1890	18
(η^2-1,4-PD)$W(CO)_4$ (alkane solid, 77 K)	~2045				~1885	18
3. *trans*-(C_2H_4)$_2Cr(CO)_4$ (Xe soln, 195 K)			1953.1			15
4. *cis*-(C_2H_4)$_2Cr(CO)_4$ (Xe soln, 195 K)	2036.8		1949.3		1913.4	15
cis-(C_2H_4)$_2Cr(CO)_4$ (gas, 295 K)	2045 (0.31)		1961 (1.00)		1931 (0.49)	14
(η^4-C_4H_6)$Cr(CO)_4$ (*n*-heptane)	2035	1979		1943	1932	12
(η^4-1,3-PD)$Cr(CO)_4$ (*n*-pentane)	2030	1964		1938	1923	29
5. (η^2-1,3-PD)$Cr(CO)_4$ (gas, 298 K)	~2013 (1.0[d])		1957 (0.85[d])		1906 (0.97[d])	*b*
(η^4-1,3-PD)$Cr(CO)_4$ (gas, 298 K)	~2050 (~0.4)	1983 (0.30)		1957 (0.84)	1949 (1.0)	*b*
6. (η^2-1,4-PD)$Cr(CO)_4$ (gas, 298 K)	~2017 (0.75[d])		1953 (1.0[d])		1920 (0.58[d])	*b*
(η^4-1,4-PD)$Cr(CO)_4$ + ($\eta^{2:CH}$-1,4-PD)$Cr(CO)_4$ (gas, 298 K)		~1970 (sh)		1953	1931	*b*
7. (η^2-COE)$Cr(CO)_5$ (heptane)	2074		1960	~1955 (sh)		17a
(η^2-C_2H_4)$Cr(CO)_5$ (pentene, 253 K)	2078 (w)		1967 (s)	1961 (vs)		17b
(η^2-C_2H_4)$Cr(CO)_5$ (gas, 295 K)	2085 (0.03)		1980 (0.82)	1975 (1.0)		14
(η^2-1,4-PD)$Cr(CO)_5$			1970			*c*

[a] PD = pentadiene; COE = cyclooctene. [b] Frequencies that were obtained in this study with TRIR. [c] Frequencies obtained in this study from FTIR. [d] Amplitudes obtained from the short time scale spectra at 2 μs. sh = shoulder, w = weak, s = strong, vs = very strong.

has a rate constant for reaction with parent of $(3.7 \pm 0.4) \times 10^{14}$ cm^3 mol^{-1} s^{-1}, which is of the same order as the gas kinetic limit for rate constants in this system (10^{14}–10^{15} cm^3 mol^{-1} s^{-1}).

B. $Cr(CO)_4$ + *trans*-1,3-Pentadiene. The reaction of $Cr(CO)_4$ with 1,3-pentadiene (1,3-PD) and 1,4-pentadiene (1,4-PD) was studied in an effort to compare the reactivity of $Cr(CO)_4$ with conjugated and nonconjugated dienes. These specific ligands were chosen because they are the smallest dienes that have both a conjugated and a nonconjugated form. This allows for a comparison of two very similar species that differ in conjugation. Additionally, since one of the species, 1,3-pentadiene, forms a stable saturated complex with $Cr(CO)_4$, it is certain that at least one reactive process can lead to formation of a stable product. For the studies involving 1,3-pentadiene, the pure trans isomer was used to avoid potential complications resulting from the reactions of an isomeric mixture of reagents.

The reactions of pentadiene with $Cr(CO)_4$ can be divided into two distinct time regimes. On time scales shorter than a few microseconds, there is initial reaction of $Cr(CO)_4$ with pentadiene, while on time scales longer than 10 μs subsequent rearrangement of the initially formed pentadiene/$Cr(CO)_4$ complex can be observed. To simplify subsequent discussion, each section dealing with pentadiene reactions has been split into four subsections based on the dominant time scale for the process under study as well as the emphasis of the study (spectroscopy and kinetics). The results from the spectroscopic studies for 1,3-pentadiene are discussed first.

1. Short Time Scale Spectra of $Cr(CO)_4$ + 1,3-Pentadiene. To follow the first step(s) in the reaction of $Cr(CO)_4$ with 1,3-pentadiene, spectral changes were monitored over the first 10 μs following photolysis. Preliminary assignments of the initial reaction products were made by comparing time-resolved IR spectra with known IR spectra of previously reported (diene)$Cr(CO)_4$ complexes. These data indicate that (η^2-1,3-PD)$Cr(CO)_4$ is formed in the first few microseconds following photolysis of $Cr(CO)_6$ in the presence of 1,3-pentadiene.

The time-resolved spectrum of the initially observed species acquired during the first 0.8 μs following the photolysis of 7 mTorr of $Cr(CO)_6$ in the presence of 0.6 Torr of *trans*-1,3-pentadiene and 7 Torr of Ar is displayed in Figure 2. In this and all subsequent TRIR spectra in this paper, the amplitudes of the product absorption bands have been expanded and the parent absorption band truncated.

Figure 2 has negative-going bands at 2000 cm^{-1} due to depletion of $Cr(CO)_6$ and at ~1970 cm^{-1} due to depletion of the small amount of naturally abundant (^{13}CO)$Cr(CO)_5$.[28] The previously discussed small $Cr(CO)_5$ band is at 1980 cm^{-1}, and three product bands that grow in at equal rates at 2013 cm^{-1} (**1**), 1957 cm^{-1} (**2**), and 1906 cm^{-1} (**3**) are diene pressure dependent, and are thus due to a (1,3-PD)/$Cr(CO)_4$ complex.

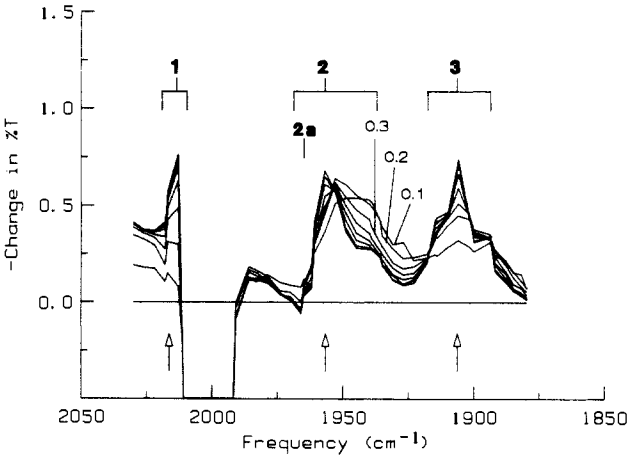

Figure 2. Time-resolved spectrum of the first 0.8 μs following photolysis of 7 mTorr of $Cr(CO)_6$ in the presence of 0.6 Torr of *trans*-1,3-pentadiene and 7 Torr of Ar. The parent depletion band at 2000 cm^{-1} has been truncated to reveal greater detail in the remaining portions of the spectrum. The eight traces in the spectrum are incremented by 0.1 μs from each other while the direction of growth at peak product absorptions is indicated by arrows. The time increments of the first three traces are indicated (in μs), while the positions of the maximum absorption bands at 2013, 1957, and 1906 cm^{-1} are labeled as **1**, **2**, and **3**, respectively. Axes are as in Figure 1.

It can be determined that this (1,3-PD)/$Cr(CO)_4$ complex is not a saturated species by comparing the positions of bands **1**, **2**, and **3** with those found in Table I for the saturated complexes: (η^4-1,3-PD)$Cr(CO)_4$ in *n*-pentane solution[29] and (C_2H_4)$_2Cr(CO)_4$ in the gas phase.[14] Bands **1** and **3** in Figure 2 are positioned lower in frequency than the corresponding high- and low-frequency absorption bands of these two saturated species. Since the gas-phase IR spectra of metal carbonyls generally absorb at higher frequencies than those in the condensed phase, bands **1** and **3** are clearly positioned *lower than expected* for either (η^4-1,3-PD)-$Cr(CO)_4$ or (η^2-1,3-PD)$_2Cr(CO)_4$. Additionally, previous gas-phase studies have shown that, in general, the IR bands of metal carbonyls shift to lower frequencies with increasing unsaturation.[21] For these reasons, this initially formed complex is assigned as the

(28) Jones, L. H.; McDowell, R. S.; Goldblatt, M. *Inorg. Chem.* **1969**, *8*, 2349.

(29) Kotzian, M.; Kreiter, C. G.; Ozkar, S. *J. Organomet. Chem.* **1982**, *229*, 29.

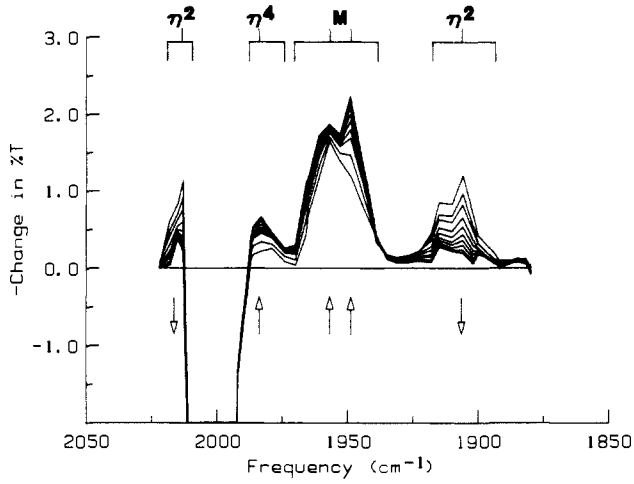

Figure 3. Time-resolved spectrum obtained over a 1.0-ms time scale by photolyzing 20 mTorr of $Cr(CO)_6$ in the presence of 0.75 Torr of 1,3-pentadiene and 6.5 Torr of Ar. Each successive trace in this figure is separated by 0.1 ms. Bands labeled η^2 are due to $(\eta^2$-1,3-PD)$Cr(CO)_4$, while η^4 indicates a band due to $(\eta^4$-1,3-PD)$Cr(CO)_4$, and **M** indicates regions where the two species overlap. The direction of growth or decay at peak absorptions is indicated by arrows. Axes are as in Figure 1.

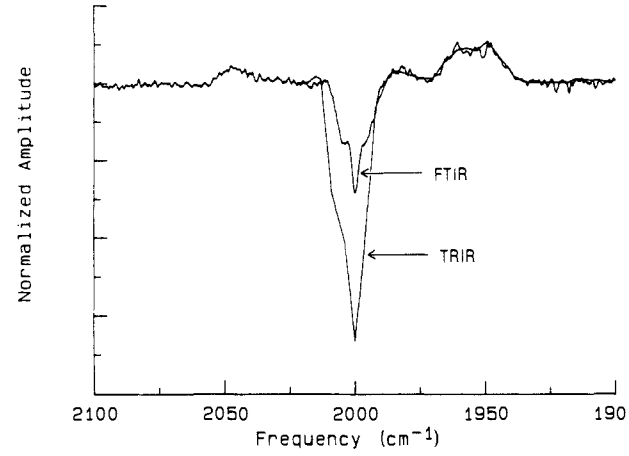

Figure 4. Overlap of FTIR and TRIR spectra. The FTIR spectrum is a single scan spectrum taken immediately following the photolysis of 50 mTorr of $Cr(CO)_6$ and 100 Torr of 1,3-pentadiene in a static cell subtracted from a spectrum of the same cell taken 25 min later. The two spectra have been normalized relative to the absorption band at 1965 cm^{-1}. The y axis is in arbitrary units while the x axis is in wavenumbers.

coordinatively unsaturated species $(\eta^2$-1,3-PD)$Cr(CO)_4$.[30] This assignment will be confirmed by kinetic studies with both 1,3- and 1,4-pentadiene.

The product bands in Figure 2 narrow and shift toward higher frequencies with time. This behavior was also noted in the spectrum of $Cr(CO)_4$ in Ar in the absence of added ligand (Figure 1), and it has been observed in a variety of other systems.[22,23] It indicates the formation of an internally excited photoproduct or reaction product. In Figure 2, this behavior implies the initial formation of internally excited $[(\eta^2$-1,3-PD)$Cr(CO)_4]^*$. Close inspection of this figure reveals that absorption band **2** appears to shift more significantly than band **3**. This is due to an overlap of absorptions of $[Cr(CO)_4]^*$ and $[(\eta^2$-1,3-PD)$Cr(CO)_4]^*$ at 1957 cm^{-1} (absorption **2** in Figure 2), which does not occur at the frequency of absorption **3**.

In Figure 2, 1,3-pentadiene is present in ~85-fold excess versus $Cr(CO)_6$. Under these conditions the reaction of $Cr(CO)_4$ with parent cannot effectively compete with the reaction of $Cr(CO)_4$ with 1,3-pentadiene. Therefore, the depletion of parent is due only to photolysis and not to reaction with $Cr(CO)_4$. Thus, the parent decay signal at 2000 cm^{-1} consists of only a single exponential detector-limited fall.

2. Long Time Scale Spectra of $Cr(CO)_4$ + 1,3-Pentadiene. Since formation of the stable complex, $(\eta^4$-1,3-PD)$Cr(CO)_4$, is not observed in the first few microseconds, the reaction mixture was monitored over a longer time period. Figure 3 shows the time-resolved spectrum that was obtained during the first millisecond following the photolysis of 20 mTorr of $Cr(CO)_6$ in the presence of 0.75 Torr of 1,3-pentadiene and 6.5 Torr of Ar.

As could be anticipated on the basis of the final trace in Figure 2, the initial trace in Figure 3 contains product absorptions at 2013, 1957, and 1906 cm^{-1} (compare with absorption bands **1**, **2**, and **3** in Figure 2). After a few tenths of a millisecond, the bands at 2013 and 1906 cm^{-1} in Figure 3, labeled η^2, decay virtually to the base line. A new band, labeled η^4, grows in at 1983 cm^{-1}. The band at 1957 cm^{-1}, labeled **M**, changes shape, increases in amplitude, and develops a new peak at 1949 cm^{-1}. That this band (**M**) does not disappear but rather changes shape and increases in amplitude implies that it contains absorptions due to both the initial (short time scale) species and the species that grows in on a longer time scale. The frequencies of the three absorptions that grow in in Figure 3 agree well with the three lowest CO-stretching band positions for $(\eta^4$-1,3-PD)$Cr(CO)_4$ in *n*-pentane solution[29] (1964, 1938, and 1923 cm^{-1}) after considering that gas-phase spectra for metal carbonyls are typically shifted 10–30 cm^{-1} higher in frequency relative to their solution-phase counterparts.[21b] It is now apparent that absorptions labeled η^2 are due to $(\eta^2$-1,3-PD)$Cr(CO)_4$, the absorption labeled η^4 is due to $(\eta^4$-1,3-PD)-$Cr(CO)_4$, and the absorption labeled **M** is due to both species. Definitive evidence that the species that grows in on the time scale of this spectrum is indeed $(\eta^4$-1,3-PD)$Cr(CO)_4$ is provided by both the FTIR and the kinetics studies discussed below.

The isobestic point in Figure 3 between 1935 and 1939 cm^{-1} implies direct rearrangement of $(\eta^2$-1,3-PD)$Cr(CO)_4$ to form the stable final product $(\eta^4$-1,3-PD)$Cr(CO)_4$. Since absorptions due solely to the $(\eta^2$-1,3-PD)$Cr(CO)_4$ decay nearly completely to base line, if an equilibrium exists between the η^2- and η^4-complexes it must lie far to the side of the stable η^4-complex. Further confirmation that the product spectrum observed in Figure 3 is due to the stable species $(\eta^4$-1,3-PD)$Cr(CO)_4$ was obtained by monitoring the photolysis products with FTIR spectroscopy. In these studies, 50 mTorr of $Cr(CO)_6$ was photolyzed with *one* laser pulse in the presence of 100 Torr of 1,3-pentadiene in a static IR cell. Product bands were observed at ~2050, ~1980, ~1960, and ~1945 cm^{-1} in a spectrum acquired ~15 s after photolysis. Not only do these band positions agree nicely with those cited above for $(\eta^4$-1,3-PD)$Cr(CO)_4$ in *n*-pentane, after considering the expected frequency shift of a gas-phase IR spectrum (see Table I), but the three lowest bands in this FTIR spectrum overlap very nicely with those of the final product in Figure 3. A comparison of the TRIR and FTIR spectra is shown in Figure 4. Furthermore, since the species observed in the FTIR spectrum (and, by implication, the species in the TRIR spectrum) has a lifetime at least as long as the ~15 s required to collect its spectrum, this species is the stable saturated complex $(\eta^4$-1,3-PD)$Cr(CO)_4$.

The FTIR spectrum displayed in Figure 4 was obtained by subtracting a spectrum acquired 25 min following photolysis from a spectrum taken immediately after photolysis. On the 25 min time scale, $(\eta^4$-1,3-PD)$Cr(CO)_4$ has decayed away (indicating that it may undergo further reactions catalyzed by the walls of the cell). Thus, the negative-going band at 2000 cm^{-1} in the FTIR spectrum is due to the increased absorbance of partially regenerated $Cr(CO)_6$ following long time decay of $(\eta^4$-1,3-PD)$Cr(CO)_4$. It is interesting to note that the amplitude of this parent recovery

(30) Unlike the spectra of $(\eta^2$-$C_2H_4)W(CO)_4$ and $(\eta^2$-$C_2H_4)_2W(CO)_4$ (see ref 18), which are very similar in solid alkane, the spectrum of $(\eta^2$-1,3-PD)-$Cr(CO)_4$ differs significantly from the spectrum of $(\eta^4$-1,3-PD)$Cr(CO)_4$ in Table I because of the presence of the band at 2013 cm^{-1}. There are two possible explanations for the discrepancy between the W and Cr systems. First, the spectra for the saturated and unsaturated Cr complexes in the gas phase may differ more dramatically than those for the saturated and unsaturated W complexes in solid alkane. Second, the 2013-cm^{-1} band in our system may not be the highest frequency band for the η^2-complex. In this case, it may correspond to one of the bands in the middle region of the spectra for the W complexes in ref 18, which were not assigned because of overlap by the parent absorption.

Scheme II

$$Cr(CO)_4 + 1,3\text{-PD} \xrightarrow{k_3} [(\eta^2\text{-}1,3\text{-PD})Cr(CO)_4]^* \quad (3)$$

$$[(\eta^2\text{-}1,3\text{-PD})Cr(CO)_4]^* + M \xrightarrow{k_4} (\eta^2\text{-}1,3\text{-PD})Cr(CO)_4 + M \quad (4)$$

$$(\eta^2\text{-}1,3\text{-PD})Cr(CO)_4 \xrightarrow{k_5} (\eta^4\text{-}1,3\text{-PD})Cr(CO)_4 \quad (5)$$

is smaller than the depletion band in the TRIR spectrum. This difference suggests that the eventual decay of $(\eta^4$-1,3-PD)Cr(CO)$_4$ does not completely lead to parent regeneration but that polynuclear species are also formed.

In summary, both the FTIR and TRIR spectroscopic results presented so far are compatible with a mechanism involving the formation of $(\eta^4$-1,3-PD)Cr(CO)$_4$ from the gas-phase addition of 1,3-pentadiene to Cr(CO)$_4$ via a sequential process: rapid addition of 1,3-pentadiene to Cr(CO)$_4$ to form $(\eta^2$-1,3-PD)Cr(CO)$_4$ (observed in Figure 2), followed by the slow conversion of $(\eta^2$-1,3-PD)Cr(CO)$_4$ to stable $(\eta^4$-1,3-PD)Cr(CO)$_4$ (observed in Figure 3). This mechanism is outlined in Scheme II (where M refers to the buffer gas).

In this mechanism, steps 3 and 4 correspond to the formation and relaxation of excited $[(\eta^2$-1,3-PD)Cr(CO)$_4]^*$ observed in the short time scale spectrum in Figure 2, while step 5 corresponds to the formation of $(\eta^4$-1,3-PD)Cr(CO)$_4$ from $(\eta^2$-1,3-PD)Cr(CO)$_4$ observed in the long time scale spectrum in Figure 3. To further test this mechanism and to determine the rate constants for each step, transient absorption signals at selected frequencies were probed while varying the pressures of the reactants. This study is described in the next two sections.

3. Kinetics of Formation of $(\eta^2$-1,3-PD)Cr(CO)$_4$. The mechanism in Scheme II can be divided in two parts according to time scale: microsecond time scale processes represented by eq 3 and 4, and millisecond time scale processes represented by eq 5. As exemplified by the short time scale spectra in Figure 2, the formation of internally relaxed $(\eta^2$-1,3-PD)Cr(CO)$_4$ (steps 3 and 4 in Scheme II) occurs in the first few microseconds or less under the conditions used in these studies (5–20 mTorr of Cr(CO)$_6$, 5 to ~50 Torr of Ar and 0.2–2 Torr of 1,3-pentadiene). To probe this process, it is desirable to monitor both the reaction of Cr(CO)$_4$ with 1,3-pentadiene (step 3 in Scheme II) and the production of relaxed $(\eta^2$-1,3-PD)Cr(CO)$_4$ (step 4 in Scheme II) as a function of reactant pressure. Unfortunately, because of spectral overlaps, there are no regions of the spectrum that contain absorptions due solely to either Cr(CO)$_4$ or $(\eta^2$-1,3-PD)Cr(CO)$_4$. Since, as described in sections III.A and III.B.1 and observed in Figures 1 and 2, interfering absorptions due to $[(\eta^2$-1,3-PD)Cr(CO)$_4]^*$ and $[Cr(CO)_4]^*$ are found in the frequency region below band **2** in Figure 2, the best choice for monitoring Cr(CO)$_4$ was the high-frequency shoulder of absorption **2** at 1965 cm^{-1}, which is labeled **2a**. The $(\eta^2$-1,3-PD)Cr(CO)$_4$ complex was also monitored at **2a** (where it overlaps with Cr(CO)$_4$) and at absorption **1** where the only convolution is due to excited CO which at this frequency is a weak absorber with a very different time dependence. Individual transient absorption signals taken at these two frequencies with 20 mTorr of Cr(CO)$_6$, 0.4 Torr of 1,3-pentadiene, and 6 Torr of Ar are shown in Figure 5.

Qualitative confirmation that the mechanism in Scheme II governs the formation of the relaxed η^2-complex can be achieved by considering the shape of the transient signal at 1965 cm^{-1} (**2a** in Figure 5). A triple-exponential signal with a rise–fall–rise is observed when P(diene) is between 0.2 and 2 Torr and P(Ar) is less than 10 Torr. This shape can be attributed to the following three steps in Schemes I and II: initial rise due to the formation of relaxed Cr(CO)$_4$ (step 1b in Scheme I); fall due to reaction of Cr(CO)$_4$ with 1,3-pentadiene (step 3 in Scheme II); and final rise due to relaxation of $[(\eta^2$-1,3-PD)Cr(CO)$_4]^*$ which forms $(\eta^2$-1,3-PD)Cr(CO)$_4$ (step 4 in Scheme II). The conspicuous time interval between the exponentials due to the second and third steps indicates that, at these pressures, the consumption of Cr(CO)$_4$ by reaction with pentadiene is faster than the formation of relaxed $(\eta^2$-1,3-PD)Cr(CO)$_4$. If the reaction of Cr(CO)$_4$ were the slower step, then the transient signal at 1965 cm^{-1} (**2a**) would appear

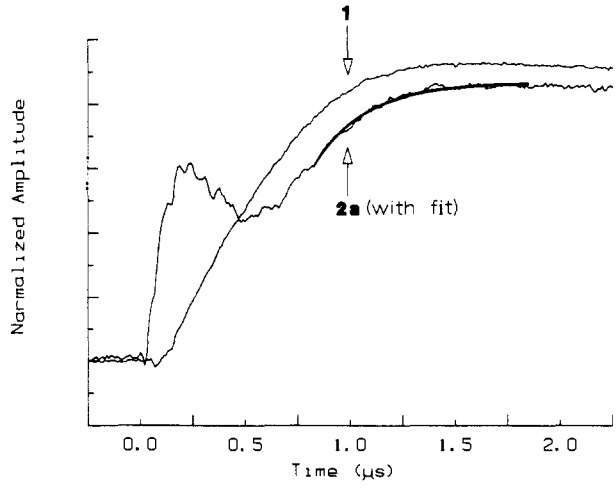

Figure 5. Overlapping signals at 2013 and 1965 cm^{-1} (labeled **1** and **2a** in accordance with designations in Figure 2) obtained with 20 mTorr of Cr(CO)$_6$, 0.4 Torr of 1,3-pentadiene, and 6 Torr of Ar. Also displayed is the best single exponential fit for the slow rise in the signal taken at **2a** in Figure 2. The y axis is in arbitrary units and the x axis in microseconds.

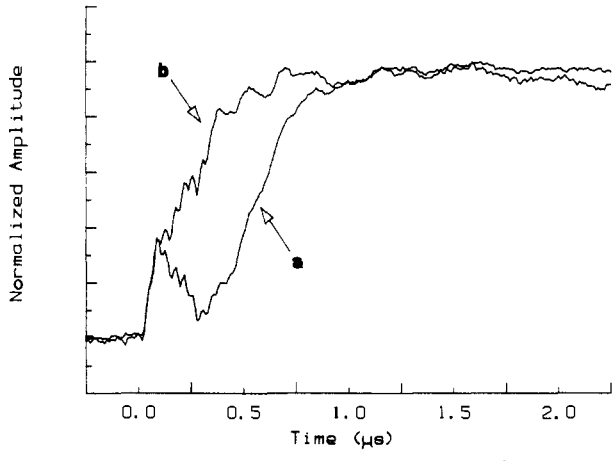

Figure 6. Comparison of the signals acquired at 1965 cm^{-1} (**2a** in Figures 2 and 5) at low and high P(Ar). Signal **a** was obtained with 12 mTorr of Cr(CO)$_6$, 1 Torr of 1,3-pentadiene, and 6 Torr of Ar. Signal **b** was obtained with 3 mTorr of Cr(CO)$_6$, 1 Torr of 1,3-pentadiene, and 21 Torr of Ar. Axes are as in Figure 5.

as a monotonic double exponential whose second rise rate would approach the rate of reaction of Cr(CO)$_4$. This assertion was confirmed by attempting to fit the signals (discussed in detail later) over a wide range of rate constants and observing that the existence of this time interval *requires* that the reaction rate of Cr(CO)$_4$ (eq 3) is significantly faster than the rate of relaxation of $[(\eta^2$-1,3-PD)Cr(CO)$_4]^*$ (eq 4).

It is also possible to experimentally confirm that the final rise of $(\eta^2$-1,3-PD)Cr(CO)$_4$ as observed at low buffer and reactant gas pressure in signals **1** and **2a** in Figure 5 is limited by the relaxation of $[(\eta^2$-1,3-PD)Cr(CO)$_4]^*$ (eq 4 in Scheme II). This is done by monitoring the rise rate of the $(\eta^2$-1,3-PD)Cr(CO)$_4$ complex at 2013 and 1965 cm^{-1} (bands **1** and **2a** in Figure 2) while increasing the Ar pressure and maintaining a constant pentadiene pressure. Initially, as the Ar pressure is increased, both rising exponentials increase in rate while the rate of the falling exponential is unaffected. As Ar pressure is increased further, the rise–fall–rise shape shown in **2a** of Figure 5 evolves into a signal with only a double-exponential rise as shown in Figure 6. Finally, at sufficiently high Ar pressures, the second of the two rising exponentials reaches a limiting rate. From this Ar pressure-dependent behavior, it is clear that the reaction of Cr(CO)$_4$ with 1,3-pentadiene (step 3 in Scheme II) becomes the rate-limiting step in the formation of relaxed $(\eta^2$-1,3-PD)Cr(CO)$_4$ when the rate of relaxation of $[(\eta^2$-1,3-PD)Cr(CO)$_4]^*$ by Ar (eq 4) surpasses

Table II. Summary of the Pentadiene Dependence of the Rate Expressions from This and Related Studies

reaction (from Scheme VII)	rate expression
(1a) $[Cr(CO)_4]^* \rightarrow Cr(CO)_4$	$k_1 = (1.1 \pm 0.6) \times 10^{14}$ cm^3 mol^{-1} s$^{-1} \times$ [PD]
(2) $Cr(CO)_4 + Cr(CO)_6 \rightarrow Cr_2(CO)_{10}$	$k_2 = (3.7 \pm 0.4) \times 10^{14}$ cm^3 mol^{-1} s^{-1}
(3i,6i) $Cr(CO)_4 + PD \rightarrow [(\eta^4\text{-PD})Cr(CO)_4]^*$	1,3-PD: $k_{3i} = (6 \pm 2) \times 10^{14}$ cm^3 mol^{-1} s^{-1} 1,4-PD: $k_{6i} = (4 \pm 2) \times 10^{14}$ cm^3 mol^{-1} s^{-1}
(4,7) $[(\eta^2\text{-PD})Cr(CO)_4]^* \rightarrow (\eta^2\text{-PD})Cr(CO)_4$	$k_4 = k_7 = (4.6 \pm 0.7) \times 10^{13}$ cm^3 mol^{-1} s$^{-1} \times$ [PD]
(5) (1,3-PD): $(\eta^2\text{-PD})Cr(CO)_4 \rightarrow (\eta^4\text{-PD})Cr(CO)_4$	$k_5 = (2.2 \pm 0.9) \times 10^3$ s^{-1}
(8) (1,4-PD): $(\eta^4\text{-PD})Cr(CO)_4 \rightarrow (\eta^{2\text{-CH}}\text{-PD})Cr(CO)_4$	$k_8 = (45 \pm 13) \times 10^3$ s^{-1} [$E_a = (11.4 \pm 0.4)$ kcal/mol]
cis-$(C_2H_4)_2Cr(CO)_4 \rightarrow (C_2H_4)Cr(CO)_4$[a]	$k = (6 \pm 2) \times 10^4$ s^{-1}
$(\eta^4\text{-}C_4H_6)Cr(CO)_4 \rightarrow (\eta^2\text{-}C_4H_6)Cr(CO)_4$[b]	$k = (2.1 \pm 0.2) \times 10^{-3}$ s^{-1}

[a] From ref 14. C_2H_4 = ethylene; reaction carried out in the gas phase at 295 K. [b] From ref 12. C_4H_6 = butadiene; reaction carried out in *n*-heptane at 300 K.

the Ar independent rate of reaction of $Cr(CO)_4$ with 1,3-pentadiene (eq 3). At these high Ar pressures, the reaction rate constant for step 3, k_3, can be estimated from the high Ar pressure rise rate of $(\eta^2$-1,3-PD)$Cr(CO)_4$.[31]

The observed rise rate for $(\eta^2$-1,3-PD)$Cr(CO)_4$ reaches a limit of 5 μs^{-1} when P(1,3-PD) = 0.2 Torr and P(Ar) $\geq$ 25 Torr, which implies a pentadiene pressure-dependent rate constant for k_3 of $\sim$25 μs^{-1} Torr^{-1} (4.6×10^{14} cm^3 mol^{-1} s^{-1}). This experimental result clearly provides evidence for the stated interpretation of the signals obtained at **2a** in Figure 2 and for validity of Scheme II and the assertion that, at Ar pressures below 10 Torr, the reaction rate of $Cr(CO)_4$ with 1,3-pentadiene (eq 3) is faster than the relaxation rate of $[(\eta^2$-1,3-PD)$Cr(CO)_4]^*$ (eq 4).

In the results presented thus far, the initial formation of $[(\eta^2$-1,3-PD)$Cr(CO)_4]^*$ (step 3 in Scheme II) and the relaxation of $[(\eta^2$-1,3-PD)$Cr(CO)_4]^*$ by buffer gas (step 4 in Scheme II) have been observed. In an attempt to quantitatively determine the diene pressure dependence of these two steps as well as to further confirm the validity of the mechanism in Scheme II, the rates of the rise–fall–rise signals obtained at low Ar pressures at band **2a** in Figure 2 (exemplified by the signal in Figure 5 taken at 1965 cm^{-1}) were investigated in more detail. Unfortunately, the rapid rise–fall–rise shape of the signals and the resulting limited number of data points did not allow for full analysis of rates k_1 through k_4 by the Provencher multiexponential fitting routine. This situation necessitated a different type of curve analysis and fitting procedure.

One of the rate constants, k_2 (the reaction rate of $Cr(CO)_4$ with $Cr(CO)_6$), could be determined independently of the rest of the rates in a system where only $Cr(CO)_6$ (and Ar) is present. As discussed in section III.A, the bimolecular rate constant for the reaction of $Cr(CO)_4$ with $Cr(CO)_6$ (k_2) is $(3.7 \pm 0.4) \times 10^{14}$ cm^3 mol^{-1} s^{-1}. To determine the rate constant for formation of relaxed $(\eta^2$-1,3-PD)$Cr(CO)_4$ (k_4), the transient absorption signals at bands **1** and **2a** in Figure 2 were monitored over a 4-fold range of 1,3-pentadiene pressures and the final rising portions of these signals were fit with a single exponential rise with use of the Provencher routine. The fit generated for this portion of the signal acquired at absorption **2a** in Figure 2 with 0.4 Torr of 1,3-pentadiene and 6 Torr of Ar is shown in Figure 5 overlapping the actual signal acquired at absorption **2a**. A plot of the single exponential rise rate of relaxed $(\eta^2$-1,3-PD)$Cr(CO)_4$ at band **2a** in Figure 2 is shown in Figure 7 as a function of diene pressure. The least-squares fit through the data gives the following expression for k_4 (at P(Ar) = 6 Torr): $(4.6 \pm 0.7) \times 10^{13}$ cm^3 mol^{-1} s$^{-1} \times$ [1,3-PD] + $(3.0 \pm 0.5) \times 10^6$ s^{-1}. As expected from the discussion on the Ar pressure dependence of this rise rate, the expression for k_4 contains a significant intercept due to the contribution of the Ar buffer gas to the relaxation of $[(\eta^2$-1,3-PD)-$Cr(CO)_4]^*$. Also, the pentadiene pressure-dependent rise rate for band **1** in Figure 2 equals, within the error limits, the value for band **2a**.

(31) Apkarian, V. A.; Weitz, E. *J. Chem. Phys.* **1979**, *71*, 4349.

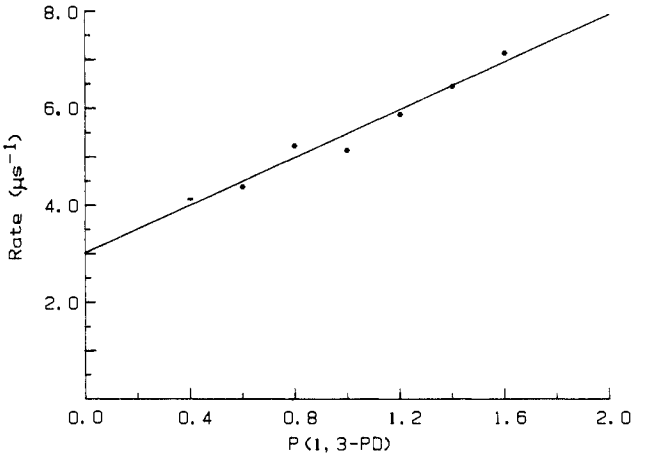

Figure 7. Plot of the rate of the slow rise portion of signals (in units of μs^{-1}) at 1965 cm^{-1} (**2a** in Figures 2 and 5) as a function of diene pressure (in Torr).

The other two rate constants, k_1 and k_3, were determined from synthesized signals with use of these rate constants for k_2 and k_4 and variable values for k_1 and k_3. The triple-exponential signals that were generated with use of variable values of k_1 and k_3 were then compared to the signals acquired at absorption **2a** in Figure 2 to determine the best values for k_1 and k_3 at low pentadiene pressures and then again at high pentadiene pressures.

The two expressions that give the best fits over the entire pressure range are $k_1 = (1.1 \pm 0.6) \times 10^{14}$ cm^3 mol^{-1} s$^{-1} \times$ [1,3-PD] + $(2,8 \pm 0.2) \times 10^6$ s^{-1} and $k_3 = (6 \pm 2) \times 10^{14}$ cm^3 mol^{-1} s^{-1}. For the diene-independent term in k_1, the relaxation rate for $[Cr(CO)_4]^*$ with 7.2 Torr of added Ar (discussed in section III.A) was used. The quoted error limits for the other terms in these two rate expressions were not determined statistically but by visual comparison of the fits to the original data. It should be noted that the value of k_3 that produced the best fit is in good agreement with the value of k_3 estimated on the basis of the previously discussed experiment done at high Ar pressure (4.6×10^{14} cm^3 mol^{-1} s^{-1}). This agreement between the value of k_3 at low Ar pressure and the experimentally determined value of k_3 at high Ar pressure also implies that k_3 is Ar pressure independent. This pressure independence was confirmed by experiments that measured the same value of k_3 at 25 and 50 Torr of Ar. This observation also implies that reaction 3 is not reversible since if it were the observed rate of depletion of $Cr(CO)_4$ (k_3) would depend on the rate of stabilization of the initially formed complex in reaction 3, which would depend on buffer gas pressure. This is not observed. These rate expressions are summarized in Table II.

It should also be noted that in the above procedure good fits were obtained by assuming that the rate constant for reaction of excited $[Cr(CO)_4]^*$ with 1,3-pentadiene equals that for relaxed $Cr(CO)_4$ with 1,3-pentadiene (k_3). Since $[Cr(CO)_4]^*$ is formed in a range of internally excited states, a rate constant for reaction

of $[Cr(CO)_4]^*$ would in itself represent an average over this distribution of states. Also, since $[Cr(CO)_4]^*$ is both relaxed by and reacts with pentadiene, a determination of the value of the rate constant for reaction of a specific internal state of $Cr(CO)_4$ with pentadiene is not possible in the present experiment. Similarly, even an accurate determination of the difference in the rate of reaction of $Cr(CO)_4$ versus $[Cr(CO)_4]^*$ with pentadiene is difficult given the overlap in the spectra of these species. Thus, explicit inclusion of the rate of reaction of $[Cr(CO)_4]^*$ in the reported kinetic schemes would only serve to complicate them without providing additional information. Therefore, the value of the rate of reaction that is reported for $Cr(CO)_4$ with pentadiene should be regarded as an "average" over both internally excited and unexcited $Cr(CO)_4$. However, there exists evidence from the studies involving the photolysis of $Cr(CO)_6$ in the absence of pentadiene that $[Cr(CO)_4]^*$ reacts with $Cr(CO)_6$ more slowly than does relaxed $Cr(CO)_4$. If the same trend is followed with pentadiene, the actual rate of reaction of $[Cr(CO)_4]^*$ with pentadiene will be slower than that of $Cr(CO)_4$ and 4.6×10^{14} cm^3 mol^{-1} s^{-1} would be a lower limit for the reaction rate of ground-state $Cr(CO)_4$ with pentadiene. However, the ground-state reaction rate cannot be much greater than this "average value" for k_3 since the observed value is already close to the gas kinetic limit. Additionally, within experimental error, k_3 is observed to be independent of the buffer gas pressure although the relative amounts of relaxed $Cr(CO)_4$ and excited $[Cr(CO)_4]^*$ are not pressure independent.

It is interesting to note that the rate of reaction of $Cr(CO)_4$ with pentadiene (k_3) is only slightly faster than the rate of reaction of $Cr(CO)_4$ with parent, $(3.7 \pm 0.4) \times 10^{14}$ cm^3 mol^{-1} s^{-1}. Similarly, Wasserman et al.[32] have observed that the photolytically produced species $(C_5H_5)Co(CO)$ reacts as rapidly with its parent molecule, $(C_5H_5)Co(CO)_2$, as it does with a variety of electron-donating ligands in both the gas and solution phases. They attribute this high reactivity to the strong Lewis basicity of the parent molecule which is also a plausible explanation for the rapid reactions in the $Cr(CO)_6$ system.

4. Kinetics of Formation of $(\eta^4$-1,3-PD)Cr(CO)$_4$. We now consider the kinetics of formation of $(\eta^4$-1,3-PD)$Cr(CO)_4$. Signals that result from depletion of $(\eta^2$-1,3-PD)$Cr(CO)_4$ (at the point labeled η^2 in Figure 3) and the growth of $(\eta^4$-1,3-PD)$Cr(CO)_4$ (at positions labeled η^4 and **M** in Figure 3) were monitored while varying both the 1,3-pentadiene and the $Cr(CO)_6$ pressures. Neither a 100-fold increase in pentadiene pressure (up to 30 Torr) nor a 5-fold increase in parent pressure affected the rate of step 5 in Scheme II. This pressure independence demonstrates that this reaction is a first-order process with a rate constant, k_5, of $(2.2 \pm 0.9) \times 10^3$ s^{-1}.

One might, a priori, expect a significant activation barrier for a slow first-order process. For example, Miller and Grant[2b] have determined that the rate constant for unimolecular decay of $(C_2H_4)_2Fe(CO)_3$ in the gas phase equals 0.04 s^{-1} at 316 K with an activation barrier of 27 kcal/mol. Whether the rate of formation of $(\eta^4$-1,3-PD)$Cr(CO)_4$ (k_5) is activated was determined by monitoring the rise *and* fall rates of the relevant reactant and product while varying the sample gas temperature from 298 to 336 K. Over the stated temperature range, an activation energy of 2 kcal/mol would result in a ~50% increase in reaction rate. However, no increase in the reaction rate was observed, which implies a negligible activation barrier (certainly less than 2 kcal/mol and probably less than 0.8 kcal/mol) and suggests that this step is rate limited by bond formation, not bond breaking.

The slow reaction rate for this virtually unactivated process implies that it is a highly entropically disfavored process. Since the activation energy is negligible, the pre-exponential of the Arrhenius expression for k_5 equals approximately 10^3 s^{-1}. Pre-exponentials for metal carbonyl reaction rate contants are typically much larger than this value. For example, Ishikawa et al.[33] monitored the activated dissociation of $(C_2H_6)W(CO)_5$ and obtained a pre-exponential factor of 10^{13} s^{-1}. The ligand rearrangement reaction of $(C_5H_5)M(CO)_2(C_2H_2)$,[14,15] studied by Kazlauskas and Wrighton,[34] yields pre-exponentials in the range 10^8–10^{10} s^{-1}. However, these reactions involve bond-breaking and ligand rearrangement, and they clearly do not involve the same restrictions on the configuration of the transition state that would be expected in the attachment of the free double bond in $(\eta^2$-1,3-PD)$Cr(CO)_4$ to the metal center. Though there are some interesting studies of the reattachment of a "loose end" of a bidentate ligand to a coordinatively unsaturated metal center,[36] these studies have been performed in solution where interaction of the coordinatively unsaturated center with solvent is important, and thus it was not possible to directly monitor the ring-closure step involving the naked coordinately unsaturated species. To our knowledge, no comparable reaction has ever been studied. Thus, even though the small pre-exponential obtained in this study might initially seem surprising, its magnitude is not unreasonable given the nature of reaction 5. Furthermore, the very fact that k_5 has a negligible activation energy and a low pre-exponential factor provides additional evidence that the conversion of unsaturated $(\eta^2$-1,3-PD)$Cr(CO)_4$ to $(\eta^4$-1,3-PD)$Cr(CO)_4$ is being observed in this reaction step.

However, since k_5 does have a small pre-exponential, an effort was made to explore alternative explanations for this slow unactivated reactive process. Other reaction mechanisms were considered that could involve a pre-equilibrium in going from the η^2- to the η^4-complex. A reaction of this type would involve an intermediate (X) as shown in eq 5a. In this mechanism, the

$$(\eta^2\text{-1,3-PD})Cr(CO)_4 \underset{k_{5r}}{\overset{k_{5f}}{\rightleftharpoons}} X \xrightarrow{k_X} (\eta^4\text{-1,3-PD})Cr(CO)_4 \qquad (5a)$$

observed rate of formation of $(\eta^4$-1,3-PD)$Cr(CO)_4$ would be slower than either of the two forward rates if the initial equilibrium lies far to the side of the reactant, $(\eta^2$-1,3-PD)$Cr(CO)_4$, i.e., k_{5r} is significantly greater than k_{5f}. This is equivalent to a situation in which application of a "steady-state" treatment for X is valid. Under these circumstances the observed first-order rate of formation of $(\eta^4$-1,3-PD)$Cr(CO)_4$ would be a composite of the three rate contants in eq 5a as follows.

$$d[(\eta^4\text{-1,3-PD})Cr(CO)_4]/dt = k_{obs}[(\eta^2\text{-1,3-PD})Cr(CO)_4] \qquad (5b)$$

$$\text{where } k_{obs} = k_{5f}k_X/(k_{5r} + k_X)$$

In eq 5b, k_{obs} is equivalent to k_5 [$(2.2 \pm 0.9) \times 10^3$ s^{-1}] and contains multiple rate constants in order to account for the small magnitude of k_5 while maintaining pre-exponentials larger than 10^3 s^{-1} for each of the rate constants in eq 5a. If k_X were approximately equal to or significantly greater than k_{5r}, eq 5b would simplify to $k_{obs} \simeq k_{5f}$. In this case, k_{obs} would equal the single rate constant (k_5), which would mean that the above discussion of the Arrhenius parameters for k_5 would still apply. To provide an alternative explanation for the small unactivated rate constant obtained for k_{obs}, a term in the denominator of eq 5b must be retained. To fulfill this condition, k_X must be significantly smaller than k_{5r}, in which case k_{obs} would simplify to the expression

$$k_{obs} = \frac{k_{5f}k_X}{k_{5r}} = \frac{A_{5f}A_X}{A_5} \exp\left(\frac{E_{5r} - E_{5f} - E_X}{RT}\right) \qquad (5c)$$

where A_i's are the pre-exponential factors and the E_i's are the activation energies for the Arrhenius expressions for the individual rate constants. Equation 5c implies that there are three requirements to ensure that the formation of $(\eta^4$-1,3-PD)$Cr(CO)_4$ from $(\eta^2$-1,3-PD)$Cr(CO)_4$ manifests itself as a first-order, unactivated process. The expression in eq 5c must be first order

(32) Wasserman, E. P.; Bergman, R. G.; Moore, C. B. *J. Am. Chem. Soc.* **1988**, *110*, 6076.
(33) Ishikawa, Y.; Brown, C. E.; Hackett, P. A.; Rayner, D. M. *Chem. Phys. Lett.* **1988**, *150*, 506.
(34) Kazlauskas, R. J.; Wrighton, M. S. *J. Am. Chem. Soc.* **1982**, *104*, 6005.
(35) Dobson, J. private communication and Zhang, S. Ph.D. Thesis, North Texas State University, 1990.
(36) Brookhart, M.; Green, M. L. H. *J. Organomet. Chem.* **1983**, *250*, 395.

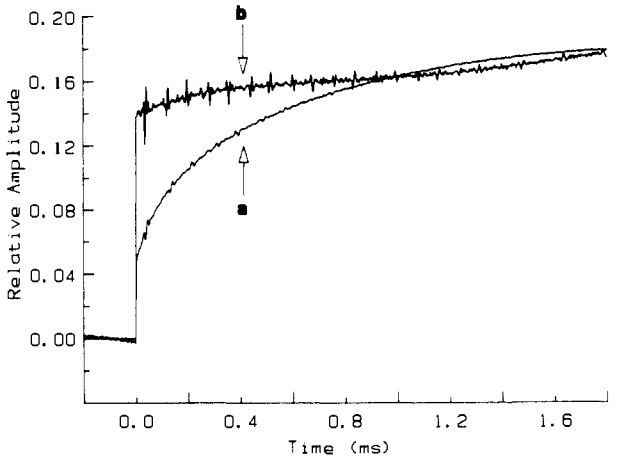

Figure 8. Comparison of the signals acquired at 1949 cm^{-1} (region **M** in Figure 3) at low and high Ar pressures. Signal **a** was obtained with 20 mTorr of $Cr(CO)_6$, 1 Torr of 1,3-pentadiene, and 8 Torr of Ar. Signal **b** was obtained with 5 mTorr of $Cr(CO)_6$, 1 Torr of 1,3-pentadiene, and 53 Torr of Ar. These signals have been divided by the intensities of the corresponding $Cr(CO)_6$ parent bands so that their amplitudes can be accurately compared. The y axis designates the fractional amplitude relative to the parent band while the x axis is in milliseconds.

(pressure independent), the observed pre-exponential ($A_{obs} = A_{5f}A_X/A_{5r}$) must equal $\sim 10^3$ s^{-1}, and the observed activation energy ($E_{obs} = E_{5r} - E_{5f} - E_X$) must be negligible. Even if we do not assume that the initial reactant in eq 5a is (η^2-1,3-PD)-$Cr(CO)_4$, we are unable to arrive at a physically reasonable intermediate, X, for the pre-equilibrium step that is compatible with these constraints. Therefore, since experimental evidence is compatible with a direct A → B process (recall the isosbestic point in Figure 3) and we are unable to provide a plausible mechanism to support a multistep conversion of (η^2-1,3-PD)$Cr(CO)_4$ to (η^4-1,3-PD)$Cr(CO)_4$, at this point there is no compelling evidence to indicate reaction 5 in Scheme II is not an elementary first-order process.

$$(\eta^2\text{-1,3-PD})Cr(CO)_4 \xrightarrow{k_5} (\eta^4\text{-1,3-PD})Cr(CO)_4 \qquad (5)$$

Studies performed at a high pressure of buffer gas indicate that in addition to the mechanism outlined in Scheme II for the two-step formation of (η^4-1,3-PD)$Cr(CO)_4$, this compound can also be formed directly from attachment of 1,3-pentadiene to $Cr(CO)_4$. This direct route was first observed by monitoring the changes in the long time scale spectra while increasing the pressure of argon.

As the Ar pressure is increased, changes in the transient absorptions indicate that (η^4-1,3-PD)$Cr(CO)_4$ is being formed rapidly at the expense of (η^2-1,3-PD)$Cr(CO)_4$. An example of the change in the transient absorption signals in the **M** region can be seen in Figure 8. The relative amplitude of the first of the two exponential rises is seen to increase with increasing Ar pressure. In the η^4 region, at high Ar pressures, the signals become rising double exponentials (where the initial exponential appears as a virtually instantaneous rise on the 2 μs time scale shown in Figure 8), which are similar in appearance to the signals seen in the **M** region. In both of these regions, the amplitude of the initial rapidly rising portion of the signal increases relative to the final amplitude (after ~2 ms) as the Ar pressure is increased. However, the *final* amplitude of the signals (after ~2 ms) remains constant over the pressure range of Ar studied. On the other hand, in the η^2 region of the spectrum, the amplitude of the (η^2-1,3-PD)$Cr(CO)_4$ complex *decreases* with increasing Ar pressure. Note that the first-order rate of formation of (η^4-1,3-PD)$Cr(CO)_4$ from (η^2-1,3-PD)Cr-$(CO)_4$, given by k_5, is constant over the range of Ar pressures studied (7–50 Torr). The rapid formation of η^4-complex is also observed at high pressures of He (up to 80 Torr) and 1,3-pentadiene (up to 30 Torr). This confirms that Ar (as well as He and diene) are not acting as reactants but as relaxers of internal energy.

Scheme III

$$Cr(CO)_4 + \text{1,3-PD} \xrightarrow{k_{3i}} \text{I}^* \qquad (3i)$$

$$\text{I}^* \xrightarrow{k_{3d}} [(\eta^2\text{-1,3-PD})Cr(CO)_4]^* \qquad (3d)$$

$$\text{I}^* + \text{M} \xrightarrow{k_{3r}} (\eta^4\text{-1,3-PD})Cr(CO)_4 + \text{M} \qquad (3r)$$

The question then arises as to how Scheme II must be modified to account for the short time production of the η^4-complex. Since the pressure-dependent amplitude change observed in Figure 8 occurs during the first few microseconds, the reaction leading to rapid formation of (η^4-1,3-PD)$Cr(CO)_4$ at the expense of (η^2-1,3-PD)$Cr(CO)_4$ at high buffer gas pressures must occur prior to step 5 in Scheme II. Furthermore, it is unlikely that the reaction leading to rapid formation of (η^4-1,3-PD)$Cr(CO)_4$ occurs during step 4 since equivalent rate increases in k_4 by Ar and 1,3-pentadiene affect the relative amounts of (η^2-1,3-PD)$Cr(CO)_4$ and (η^4-1,3-PD)$Cr(CO)_4$ formed during the first few microseconds differently. Specifically, the same relaxation rate for [(η^2-1,3-PD)$Cr(CO)_4$]* (step 4) can be achieved with either ~2 Torr of 1,3-pentadiene or ~20 Torr of Ar. However, while increasing the diene pressure to 2 Torr causes no observable change in relative amounts of (η^2-1,3-PD)$Cr(CO)_4$ and (η^4-1,3-PD)$Cr(CO)_4$ formed during the first 2 μs, increasing the Ar pressure to 20 Torr causes an ~50% decrease in the amount of (η^2-1,3-PD)$Cr(CO)_4$ formed relative to (η^4-1,3-PD)$Cr(CO)_4$ during this same time period. Therefore, the reaction leading to rapid formation of (η^4-1,3-PD)$Cr(CO)_4$ must occur prior to step 4 in Scheme II, namely, in step 3. Up to now, this reaction step has been designated as the formation of [(η^2-1,3-PD)$Cr(CO)_4$]* from the addition of 1,3-pentadiene to $Cr(CO)_4$. Given the above observations, step 3 can no longer be considered a single elementary process since it involves the formation of *both* [(η^2-1,3-PD)$Cr(CO)_4$]* and (η^4-1,3-PD)$Cr(CO)_4$. To adequately account for these results, step 3 must be expanded into a reaction with two branches that involve a common intermediate. This is shown in Scheme III (where M refers to buffer gas).

This scheme adequately accounts for the branched reaction leading to direct formation of (η^4-1,3-PD)$Cr(CO)_4$ without altering the rest of the mechanism. Reaction 3i is the addition of pentadiene to $Cr(CO)_4$, whose rate constant (formerly just k_3) was discussed in section III.B.3. Reaction 3d is the bond scission step, which is the dominant step for I* depletion at low buffer gas pressures, while reaction 3r is the collisional relaxation step, which is the dominant path for I* depletion at high pressures. The behavior of I* suggests that it is a highly internally excited [(η^4-1,3-PD)$Cr(CO)_4$]* complex, which can relax by bond scission to form [(η^2-1,3-PD)$Cr(CO)_4$]* or be collisionally relaxed to form (η^4-1,3-PD)$Cr(CO)_4$.

Since reactions 3d and 3r are not rate limiting at either low buffer gas pressures (below 25 Torr, where reaction 3d predominates, but reaction 4 is rate limiting) or high buffer gas pressures (above 25 Torr, where reaction 3r predominates and reaction 3i is rate limiting), the intermediate complex, I*, is not directly observable. To better understand the nature of this intermediate, its behavior can be contrasted with that of (η^4-1,3-PD)$Cr(CO)_4$ and (η^2-1,3-PD)$Cr(CO)_4$. Unlike (η^4-1,3-PD)$Cr(CO)_4$, for which there is no evidence of dissociation to (η^2-1,3-PD)$Cr(CO)_4$ (see section III.B.2), I* can rapidly rearrange to form (η^2-1,3-PD)-$Cr(CO)_4$ (reaction 3d). The rate of this rearrangement (k_{3d}) can be estimated by monitoring the change in amplitude of the (η^2-1,3-PD)$Cr(CO)_4$ signal as a function of Ar pressure and following the competition between reactions 3d and 3r. The amplitude of the (η^2-1,3-PD)$Cr(CO)_4$ signal (band **1** in Figure 2) is reduced by approximately half when the Ar pressure is increased from 6 to 25 Torr. This implies that roughly equal amounts of the η^2- and η^4-complexes are initially formed with 25 Torr of Ar and that $k_{3d} \cong k_{3r}(M)$ (Scheme III) at this pressure. From the approximate value of the Ar contribution to the relaxation rate of k_4 at 25 Torr (see section III.B.3), it can be estimated that the rate for the relaxation reaction 3r is ~10 μs^{-1}

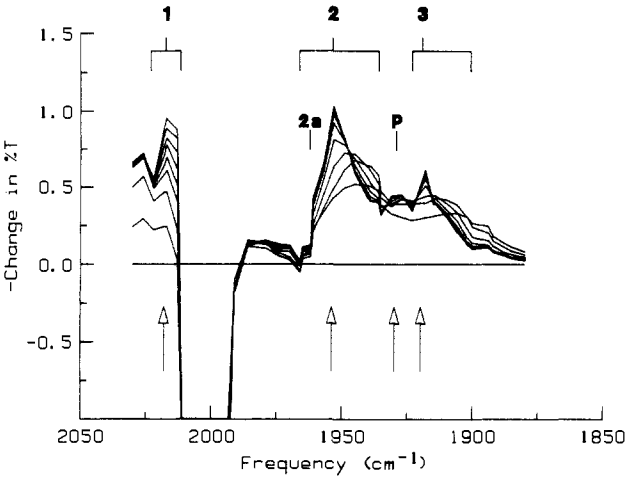

Figure 9. Time-resolved spectrum following the photolysis of 7 mTorr of $Cr(CO)_6$ in the presence of 0.5 Torr of 1,4-pentadiene and 7 Torr of Ar. The spectrum covers 0.8 μs, with each trace incremented by 0.1 μs. The direction of change in absorption is indicated by arrows. The positions of the maximum absorption bands at 2017, 1953, and 1920 cm^{-1} are labeled as **1**, **2**, and **3**, respectively. The absorptions and the small absorption labeled **P** are assigned in the text. Axes are as in Figure 2.

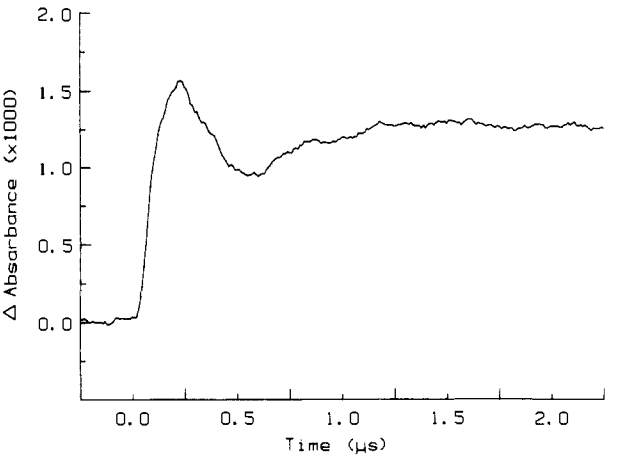

Figure 10. Transient absorption signal at 1965 cm^{-1} (**2a** in Figure 9) from photolysis of 7 mTorr of $Cr(CO)_6$, 0.6 Torr of 1,4-pentadiene, and 6 Torr of Ar. The x axis is as in Figure 5 while the y axis is now in absorbance units.

at this Ar pressure. Thus, k_{3d} (the rate of bond scission in **I***) must also equal $\sim 10\ \mu s^{-1}$. This rate is at least eight orders of magnitude faster than bond cleavage in $(\eta^4\text{-1,3-PD})Cr(CO)_4$, which, as discussed in section III.B.2, must have a lifetime at least as long as the 15 s required to take its FTIR spectrum. In contrast to $(\eta^2\text{-1,3-PD})Cr(CO)_4$, which undergoes a slow first-order, pressure-independent conversion to $(\eta^4\text{-1,3-PD})Cr(CO)_4$ (reaction 5 in Scheme II), **I*** relaxes to $(\eta^4\text{-1,3-PD})Cr(CO)_4$ via a rapid, bimolecular, pressure-dependent reaction pathway (3r in Scheme III). Therefore, although it is convenient to refer to **I*** as $[(\eta^4\text{-1,3-PD})Cr(CO)_4]^*$ since it can collisionally relax to form $(\eta^4\text{-1,3-PD})Cr(CO)_4$ or partially dissociate to form $(\eta^2\text{-1,3-PD})Cr(CO)_4$, it may be better to picture **I*** as a loosely bound 1,3-PD/$Cr(CO)_4$ complex that is held together by the electron-donating ability of 1,3-pentadiene and the strong electrophilicity of $Cr(CO)_4$.[32]

It is tempting to contrast the rapid formation of $(\eta^4\text{-1,3-PD})Cr(CO)_4$ at high buffer gas pressures (step 3r in Scheme III) with the relatively slow addition of the unattached ethylene bond in $(\eta^2\text{-1,3-PD})Cr(CO)_4$ (step 5 in Scheme II). Although constraints on the transition state lead to a slow rearrangement of $(\eta^2\text{-1,3-PD})Cr(CO)_4$ to $(\eta^4\text{-1,3-PD})Cr(CO)_4$, there is no such hindrance to the direct formation of $(\eta^4\text{-1,3-PD})Cr(CO)_4$ via rapid relaxation of $[(\eta^4\text{-1,3-PD})Cr(CO)_4]^*$. However, it is important to remember that this apparent difference is the result of comparing a bimolecular reaction of an excited complex with a unimolecular reaction of a relaxed intermediate. The route leading to rapid formation of $(\eta^4\text{-1,3-PD})Cr(CO)_4$ involves the bimolecular relaxation of highly excited $[(\eta^4\text{-1,3-PD})Cr(CO)_4]^*$ by buffer gas and is only observed when the pressure-dependent rate (k_{3r}) is increased dramatically at high buffer gas pressures so that it is competitive with k_{3d}. In contrast, the rearrangement of $(\eta^2\text{-1,3-PD})Cr(CO)_4$ involves the unimolecular conversion of a relaxed metastable intermediate rather than the collisional relaxation of a highly excited complex.

To compare the results above for the reaction of $Cr(CO)_4$ and conjugated pentadiene with the reactivity of $Cr(CO)_4$ toward a nonconjugated diene, we turn to the reaction of $Cr(CO)_4$ with 1,4-pentadiene.

C. $Cr(CO)_4$ + 1,4-Pentadiene. In this section, results are presented which demonstrate that the reaction of 1,4-pentadiene with $Cr(CO)_4$ follows a significantly different mechanism than that seen for the reaction of 1,3-pentadiene with $Cr(CO)_4$. This difference is not manifested in the early stages of the reaction (eqs 3 and 4 in Scheme II) but in the longer time scale steps (>10 μs). Since the short time scale mechanism for addition of 1,4-pentadiene to $Cr(CO)_4$ is similar to that seen in the 1,3-pentadiene system, the short time scale results will be briefly presented before devoting the major portion of the discussion to the long time scale mechanism.

Scheme IV

$$Cr(CO)_4 + \text{1,4-PD} \xrightarrow{k_6} [(\eta^2\text{-1,4-PD})Cr(CO)_4]^* \quad (6)$$

$$[(\eta^2\text{-1,4-PD})Cr(CO)_4]^* + M \xrightarrow{k_7} (\eta^2\text{-1,4-PD})Cr(CO)_4 + M \quad (7)$$

1. Short Time Scale Spectra for $Cr(CO)_4$ + 1,4-Pentadiene. The spectrum displayed in Figure 9 was obtained during the first 0.8 μs following KrF laser photolysis of 7 mTorr of $Cr(CO)_6$ in the presence of 0.5 Torr of 1,4-pentadiene and 7 Torr of Ar and is very similar to that seen at low pressure in the 1,3-pentadiene system (Figure 2). In addition to the small absorption at $\sim$1980 cm^{-1} due to $Cr(CO)_5$, four product bands can be observed at 2013, 1953, 1931, and 1920 cm^{-1} (labeled **1**, **2**, **P**, and **3** in Figure 9, respectively). The positions and behavior of bands **1**, **2**, and **3** in Figure 9 are quite similar to those in the 1,3-pentadiene spectra in Figure 2 and are assigned to $(\eta^2\text{-1,4-PD})Cr(CO)_4$. The formation of an η^2-1,4-PD complex is confirmed in the long time scale kinetic studies discussed in section III.C.4, below. The 4th band at 1931 cm^{-1} (labeled **P**) has been determined from the long time scale studies to be due to another product (discussed in section III.C.4). It can be seen that the first trace in Figure 9, taken at 0.1 μs following the laser pulse, has a broad product absorption extending from 1970 to 1900 cm^{-1}, which narrows and shifts with time, eventually resulting in the three absorptions labeled **2**, **P**, and **3**. This narrowing and shifting of the spectrum is again attributed to the internal relaxation of the initially formed species. Absorption **1** at 2013 cm^{-1} does not exhibit obvious narrowing and shifting since it overlaps with the large parent absorption.

2. Short Time Scale Kinetics for $Cr(CO)_4$ + 1,4-Pentadiene. The similarity of the short time scale spectra for the reaction of 1,3- and 1,4-pentadiene (Figures 2 and 9) suggests that the short time scale reaction mechanism in Scheme II that leads to formation of $(\eta^2\text{-1,3-PD})Cr(CO)_4$ is quite similar to the corresponding mechanism in the 1,4-pentadiene system. The analogous mechanism is shown in Scheme IV. To verify this mechanism and to probe the reaction rates for eqs 6 and 7, selected frequencies in the spectrum in Figure 9 were monitored while varying the pressures of 1,4-pentadiene and Ar buffer. Absorptions **1** and **2a** in Figure 9 were probed for the same reason that absorptions **1** and **2a** in Figure 2 were probed in the 1,3-pentadiene system: namely, to avoid the convolutions from the $[Cr(CO)_4]^*$ and $[(\eta^2\text{-PD})Cr(CO)_4]^*$ absorptions observed at frequencies below absorption **2** in Figures 2 and 9. A discussion of a branched reaction in step 6 (analogous to the one outlined in Scheme III for 1,3-pentadiene) will be deferred to allow us to focus on the reactions indicated above in eqs 6 and 7.

A transient obtained at 1965 cm^{-1} (**2a** in Figure 9) following KrF photolysis of 7 mTorr of $Cr(CO)_6$ in the presence of 0.6 Torr of 1,4-pentadiene and 6 Torr of Ar is shown in Figure 10. Following the reasoning used to explain the rise–fall–rise shape of signal **2a** in Figure 5 in the 1,3-pentadiene system, the shape of the signal in Figure 10 can be explained by a similar three-step process: (1) formation of relaxed $Cr(CO)_4$ (step 1b in Scheme I), (2) reaction of $Cr(CO)_4$ with 1,4-pentadiene (step 6 in Scheme IV) and (3), collisional relaxation of $[(\eta^2\text{-}1,4\text{-PD})Cr(CO)_4]^*$ to form $(\eta^2\text{-}1,4\text{-PD})Cr(CO)_4$ (step 7 in Scheme IV). Confirmation that the final step in the formation of $(\eta^2\text{-}1,4\text{-PD})Cr(CO)_4$ is due to the collisional relaxation of $[(\eta^2\text{-}1,4\text{-PD})Cr(CO)_4]^*$ was again achieved by monitoring the rise rate of absorptions **1** and **2a** in Figure 9 while increasing the pressure of Ar. As seen in the 1,3-pentadiene system (Figure 6), the rise rate of the $(\eta^2\text{-}1,4\text{-PD})Cr(CO)_4$ absorptions (**1** and **2a** in Figure 9) increases with increasing Ar pressure, until it reaches a limit of $\sim 5\ \mu s^{-1}$ with 0.2 Torr of 1,4-pentadiene and 25 Torr or more of Ar. As with 1,3-pentadiene, at high Ar pressures the addition of pentadiene to $Cr(CO)_4$ (step 6) becomes the rate-limiting step in the formation of internally relaxed $(\eta^2\text{-}1,4\text{-PD})Cr(CO)_4$. From this rise rate and the diene pressure, it is possible to estimate the rate constant for step 6 in Scheme IV (k_6) as 25 μs^{-1} $Torr^{-1}$ (4.6×10^{14} cm^3 mol^{-1} s^{-1}).[31] As with 1,3-pentadiene, this step is Ar pressure independent in this pressure region. The same value of k_6 was obtained at both 25 and 50 Torr of Ar.

This rate constant and the overall mechanism in Scheme IV were further confirmed by fitting triple-exponential curves to the rise–fall–rise signals (such as that in Figure 10) obtained at absorption **2a** in Figure 9 with use of the method developed for the 1,3-pentadiene system (section III.B.3). These triple-exponential curves could be fit by using the same rate expressions for $[Cr(CO)_4]^*$ relaxation (k_1), $Cr(CO)_4$ reaction with $Cr(CO)_6$ (k_2), and $[(\eta^2\text{-PD})Cr(CO)_4]^*$ relaxation (k_4, k_7) that were used in the 1,3-pentadiene fits (see Table II). The only rate expression used in these fits that differs from those of the 1,3-pentadiene system is the rate constant for reaction of $Cr(CO)_4$ with pentadiene (k_6). The value for k_6 that best fits the data is $(4 \pm 2) \times 10^{14}$ cm^3 mol^{-1} s^{-1}, which is slightly smaller than the $(6 \pm 2) \times 10^{14}$ cm^3 mol^{-1} s^{-1} value determined for reaction 3 in the 1,3-pentadiene system (k_3). Although k_6 and k_3 are equal within the error limits, close comparison of the quality of fit of signals generated while varying the values for k_6 and k_3 reveals that the best fits are obtained when the rate constant for the 1,4-pentadiene reaction (k_6) is smaller than that for the 1,3-pentadiene reaction (k_3).

Since k_3 is comparable to k_6, the reactivity of $Cr(CO)_4$ toward pentadiene during the first few microseconds does not depend strongly on diene conjugation. In both systems, the reaction of $Cr(CO)_4$ with diene occurs at near gas kinetic rates leading to a $[(\eta^2\text{-PD})Cr(CO)_4]^*$ complex, while the diene dependence of the relaxation rate of this $[(\eta^2\text{-PD})Cr(CO)_4]^*$ complex (k_4, k_7) is ~ 10 times slower. However, a significant difference in the reaction mechanism of these two dienes is observed on a longer time scale.

3. Long Time Scale Spectra for $Cr(CO)_4$ + 1,4-Pentadiene. The spectrum acquired 100 μs after KrF excimer laser photolysis of 17 mTorr of $Cr(CO)_6$ in the presence of 0.5 Torr of 1,4-pentadiene and 6.7 Torr of Ar is shown in Figure 11. Only a single time-resolved spectrum is shown because the changes observed in the spectrum on time scales longer than 10 μs are too subtle to discern without inspecting individual transient absorption signals.

This spectrum can be divided into two types of absorptions labeled **A** and **M**. In sections III.C.1 and III.C.2, the two bands in region **A** (bands **A** and **A1**) were assigned to $(\eta^2\text{-}1,4\text{-PD})Cr(CO)_4$ by analogy with the 1,3-pentadiene system (cf. Figures 2 and 9). However, to avoid biasing the kinetics discussion, the species in this region will tentatively be referred to simply as "*A*". The kinetic results will then be used to reinforce the assignment of *A* as $(\eta^2\text{-}1,4\text{-PD})Cr(CO)_4$. By inspecting individual transients, it can be determined that the middle region of the spectrum, labeled **M** in Figure 11, contains absorptions due not only to *A* but also to two other species whose reactivity differs from that of *A*. Species *A* does not undergo any further reactions after the first few microseconds, whereas the other species that absorb in region **M** continue to react throughout the first $\sim 100\ \mu s$. In all regions of the spectrum, no change in absorbance was detected after the first 100 μs. In contrast to what is observed for 1,3-pentadiene, formation of stable $(\eta^4\text{-}1,4\text{-PD})Cr(CO)_4$ *does not* occur. No stable $(\eta^4\text{-}1,4\text{-PD})Cr(CO)_4$ can be observed in an FTIR spectrum of the system taken ~ 15 s after photolyzing 50 mTorr of $Cr(CO)_6$ in the presence of 300 Torr of 1,4-pentadiene. In this FTIR spectrum, the only bands observed in the CO stretching region were those at 2000 cm^{-1} belonging to $Cr(CO)_6$.

In a further attempt to observe stable products in the FTIR spectrum, 10 Torr of CO was added to a mixture of 50 mTorr of $Cr(CO)_6$ and 300 Torr of 1,4-pentadiene. The FTIR spectrum taken 15 s after photolysis showed, in addition to the $Cr(CO)_6$ parent depletion at 2000 cm^{-1}, the growth of an absorption at 1970 cm^{-1}. A second spectrum taken 30 min later showed loss of this 1970-cm^{-1} absorption and partial recovery of the parent. To clearly display the absorbance changes at 2000 and 1970 cm^{-1}, the initial spectrum has been subtracted from the final spectrum and plotted in Figure 12. The single strong absorption at 1970 cm^{-1} is assigned as due to $(\eta^2\text{-diene})Cr(CO)_5$ since this absorption matches the IR spectrum obtained for this species in both the gas[14] and condensed phases.[17] Another band, expected at ~ 2080 cm^{-1},

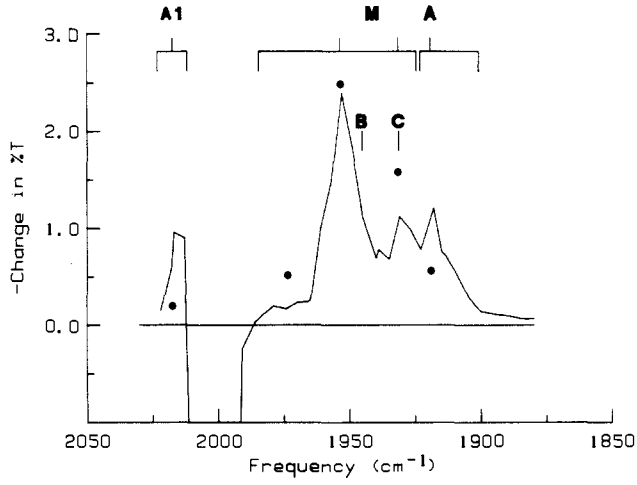

Figure 11. Transient spectrum acquired 100 μs after the photolysis of 17 mTorr of $Cr(CO)_6$ in the presence of 0.5 Torr of 1,4-pentadiene and 6.7 Torr of Ar. A solid circle (●) indicates the amplitude of signals taken at selected frequencies when $P(Ar)$ was increased to 50 Torr. Assignments of peaks are discussed in the text. Axes are as in Figure 1.

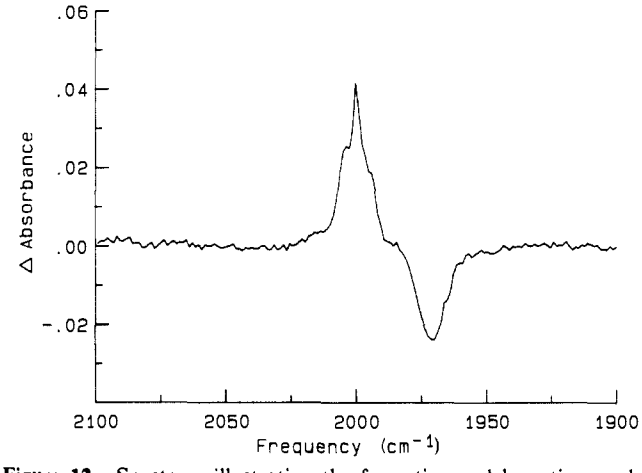

Figure 12. Spectrum illustrating the formation and long time scale degradation of $(\eta^2\text{-}1,4\text{-PD})Cr(CO)_5$. A single-scan FTIR spectrum was taken immediately following the photolysis of 50 mTorr of $Cr(CO)_6$ with 300 Torr of 1,4-pentadiene and 10 Torr of CO in a static cell. This spectrum was subtracted from a spectrum of the same cell taken 30 min later. The result is displayed in the figure. See text for further discussion of assignments.

is too weak to observe in this spectrum. The formation of this compound is consistent with the absence of a stable η^4- or, as discussed below, bis-diene product since CO adds to the (η^2-1,4-PD)$Cr(CO)_4$ species to form (η^2-1,4-PD)$Cr(CO)_5$. Interestingly the formation of (η^2-1,4-PD)$Cr(CO)_5$ was not observed on a millisecond time scale. Thus, though it occurs, this reaction is slow relative to the addition reactions of dienes. It should be noted that (η^2-1,4-PD)$Cr(CO)_5$ is *only* observed following photolysis of $Cr(CO)_6$ in the presence of both pentadiene and CO. Thus this product is not merely the result of reaction of pentadiene with the small amount of nascent $Cr(CO)_5$ produced on photolysis.

It should also be noted that, in the FTIR experiment, the formation of a stable (η^2-1,4-PD)$_2Cr(CO)_4$ complex is not observed despite the 30-fold excess pressure of 1,4-pentadiene relative to CO. This reluctance to form a stable *cis*-(PD)$_2Cr(CO)_4$ complex is borne out by solution-phase experiments, where *trans*-(η^2-olefin)$_2Cr(CO)_4$ (formed from the photolysis of *cis*-(η^2-olefin)$_2Cr(CO)_4$) is found to be stable, but the cis isomer is not.[17b] Grevels et al.[17c] attribute the lower stability of the cis isomer to competitive back-bonding between the olefin and the CO ligand trans to it in *cis*-(olefin)$_2Cr(CO)_4$.

4. Long Time Scale Kinetics for $Cr(CO)_4$ + 1,4-Pentadiene. On the basis of the long time scale (>10 μs) kinetic studies, a mechanism for the addition of 1,4-pentadiene to $Cr(CO)_4$ can be constructed that involves three (1,4-PD)$Cr(CO)_4$ species and accounts for the lack of a stable complex in this system.

Secondary reactions of the (1,4-PD)$Cr(CO)_4$ complexes that take place on time scales longer than a few microseconds can be most conveniently observed at the two frequencies labeled **B** (secondary fall) and **C** (secondary rise) in Figure 11. However, even at these frequencies, the change in amplitude in the transient absorption signals due to these reactions is less than 20%. The species that generate these absorptions will be referred to as "*B*" and "*C*". Species *A* was monitored at two positions. These are labeled **A** and **A1** in Figure 11. Unlike the transient at **A** the transient at **A1** decays, reaching a non-zero base line within 100 μs. As previously discussed (see section III.A), vibrationally excited CO (CO*) is observed above 2010 cm^{-1}. The asymmetric decay of the transient at **A1** on a 100 μs time scale can be attributed to CO* relaxation for two reasons. First, unlike the transient signals at **B** and **C**, the rate of decay at **A1** (2013 cm^{-1}) is dependent on CO pressure and has the same temporal profile as CO transients at higher frequencies than 2013 cm^{-1}. Second, the rate of the single-exponential decay of the transient taken at **A1** is different than and ~50% larger than the secondary reaction rate observed for bands **B** and **C** at room temperature. Following this 100-μs decay, the resulting base line does not decay further on a time scale of milliseconds. Therefore, species *A* is overlapped by CO* at **A1** and does not undergo a secondary reaction on this time scale.

The rate of the signals obtained at absorptions **B** and **C** (which could be fit with single exponentials) does not depend on the pressures of pentadiene, $Cr(CO)_6$, Ar, or CO. The diene pressure was varied by 200-fold, $P[Cr(CO)_6]$ by ~2-fold, and P(Ar) by 7-fold, and P(CO) was increased from 0 to 10 Torr without observing any significant change in the fall rate at **B** (1945 cm^{-1}) or rise rate at **C** (1931 cm^{-1}). The single-exponential fall rate at **B** of (45 ± 13) × 10^3 s^{-1} equals the single exponential rise rate at **C**. This behavior is characteristic of a first-order reaction of species *B* to *C*.

To determine whether this first-order process is activated, the long time scale behavior of absorptions **B** and **C** was monitored over a temperature range of 25–60 °C. Over this temperature range there was an almost 8-fold increase in the reaction rate. An Arrhenius plot of ln (k) vs $1/T$ (monitored at **C**) yields an activation energy (E_a) of (11.4 ± 0.4) kcal/mol with a pre-exponential factor of (8^{+8}_{-4}) × 10^{12} s^{-1}. Note that this pre-exponential factor is nearly 10^{10} times that determined for the slow unactivated secondary reaction observed in the 1,3-pentadiene system (step 5 in Scheme II). This contrast in pre-exponentials and the existence of a significant activation energy imply that the conversion of *B* to *C* differs significantly from the long time scale formation of (η^4-1,3-PD)$Cr(CO)_4$ from (η^2-1,3-PD)$Cr(CO)_4$.

Scheme V

$$Cr(CO)_4 + \text{1,4-PD} \xrightarrow{k_{6i}} I'^* \quad (6i)$$

$$I'^* \xrightarrow{k_{6d}} A^* \quad (6d)$$

$$I'^* + M \xrightarrow{k_{6r}} B + M \quad (6r)$$

$$[(\eta^2\text{-1,4-PD})Cr(CO)_4]^* + M \xrightarrow{k_7} (\eta^2\text{-1,4-PD})Cr(CO)_4 + M \quad (7)$$

$$B \xrightarrow{k_8} C \quad (8)$$

In light of the fact that *B* reacts to form *C*, it is useful to consider why the observed changes in the long time scale spectra in Figure 11 are so subtle. It must be that either (1) species *B* and *C* have very similar spectra or (2) their spectra differ significantly, but their concentrations change little during the reaction, implying that an equilibrium exists between *B* and *C* as shown in reactions 8_f and 8_r.

$$B \underset{k_r}{\overset{k_f}{\rightleftharpoons}} C \quad (8_f, 8_r)$$

If an equilibrium exists where $k_f \sim k_r$ and the activation energy for k_f, E_f, is significantly different than E_r, the activation energy for the reverse step, then the equilibrium will shift with temperature. This would lead to a change in the amplitude of the secondary rise of *C* with temperature. This is not observed. From the invariance in the amplitude of the rise of *C* it can be determined that if $k_f \sim k_r$ then E_f is within ~5% of E_r. However, as shown below *B* and *C* are isomers of mono-(1,4-PD)$Cr(CO)_4$ with different bonding properties, which implies that, while their IR spectra may be very similar, the activation energies for the forward and reverse isomerization reactions (8_f, 8_r) most likely are *not* equal. From these considerations, we conclude that case 1 is more likely to account for the observed behavior. Thus reaction 8 can be treated as a unimolecular conversion of *B* to *C* where the spectra of the two species strongly overlap.

As previously stated, secondary reactions were not observed for *A*. Its role in the overall reaction mechanism was determined by monitoring the pressure dependence of the relative amplitudes of *A*, *B*, and *C* at selected frequencies in both the **A** and **M** regions of the spectrum in Figure 11. In this figure, a dot at a given frequency indicates the amplitude of the signal obtained at that frequency 100 μs after photolysis of 17 mTorr of $Cr(CO)_6$ in the presence of 0.5 Torr of $Cr(CO)_6$ and at a higher (50 Torr) pressure of Ar. The major change from the spectrum obtained with 7 Torr of Ar is that the amplitudes of the bands in region **A** have decreased while those in region **M** have increased.[37] It should be noted that the reaction rates of the transients obtained at **B** and **C** are unaffected by increasing the buffer gas pressure and that the amplitudes of both of the rising exponentials at **C** increase in a fixed ratio. It should also be noted that the amplitude increases at **B** and **C** can be induced by high 1,4-pentadiene pressures. Thus, these amplitude increases are induced not by the presence of a specific reactant but by increased buffer gas pressure. This observation implies that, as in the 1,3-pentadiene system, there is a reaction with at least two branches where the relative amplitudes of the products depend on the pressure of the buffer gas. In summary, formation of *A* occurs at the expense of *B* and *C* at low buffer gas pressures and formation of *B* and *C* occurs at the expense of *A* at high buffer gas pressures.

By using these spectroscopic and kinetic results, a mechanism for the reaction of 1,4-pentadiene with $Cr(CO)_4$ can be deduced which by analogy with the 1,3-pentadiene mechanism (Scheme III) involves the initial formation of an excited species, I'^*, which can rearrange to form A^* or is collisionally relaxed to form *B*. A^* then relaxes to *A*, and *B* can convert to *C* as shown in Scheme V (where M refers to buffer gas). We now consider plausible

(37) The change in amplitude in the **M** region is not as large as in the **A** region since **M** contains absorptions due to *A* as well as *B* and *C*.

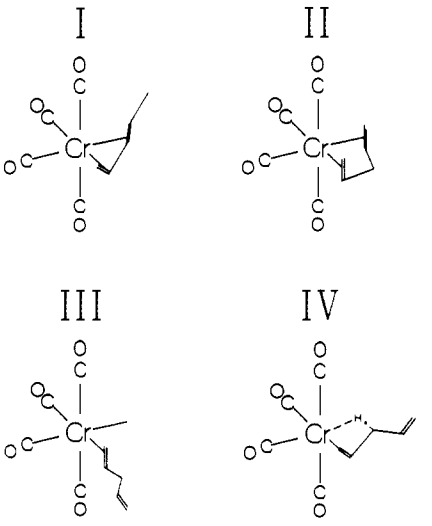

Figure 13. Likely structures for (I) (η^4-1,3-PD)$Cr(CO)_4$, (II) (η^4-1,4-PD)$Cr(CO)_4$, (III) (η^2-1,4-PD)$Cr(CO)_4$, and (IV) ($\eta^{2:CH}$-1,4-PD)$Cr(CO)_4$.

assignments for these three species.

It can be shown that neither *A*, *B*, nor *C* is (1,4-PD)$_2Cr(CO)_4$ and thus that the three most likely structures for the complexes involved in Scheme V are three isomers of mono-(1,4-PD)$Cr(CO)_4$. First, if *A* or *B* were bis-substituted (1,4-PD)$_2Cr(CO)_4$, then I'* would have to be [(1,4-PD)$_2Cr(CO)_4$]*. Otherwise, if I'* were a mono-PD complex, one of the reactions of I'* (6d or 6r) would involve the addition of a second diene to mono-(1,4-PD)$Cr(CO)_4$ to form bis-(1,4-PD)$_2Cr(CO)_4$, thus changing the relative amplitudes between *A* and *B* at low as well as high pentadiene pressures. However, *B* was observed to increase relative to *A* only at diene pressures above 10 Torr. (Perhaps more significantly, this also occurs at high Ar pressure.) Thus, if either *A* or *B* is (1,4-PD)$_2Cr(CO)_4$, I'* must be [(1,4-PD)$_2Cr(CO)_4$]*. But it is very unlikely that I'* could be [(1,4-PD)$_2Cr(CO)_4$]* since it would be the product of two sequential bimolecular addition reactions whose second step is not observable. It would also be a species with no analogy in the 1,3-pentadiene system (where we observed direct formation of (η^4-1,3-PD)$Cr(CO)_4$, not (η^2-1,3-PD)$_2Cr(CO)_4$, from the intermediate analogous to I'*). Therefore, since I'* is not [(1,4-PD)$_2Cr(CO)_4$]*, *A* and *B* are mono-olefin complexes. Finally, *C* cannot be (1,4-PD)$_2Cr(CO)_4$ since it is the product of a unimolecular rearrangement of *B*, which has just been shown to be a mono-(1,4-PD)$Cr(CO)_4$ complex. Therefore, each of the three species must be an isomer of (1,4-PD)$Cr(CO)_4$.

Two obvious isomeric structures for these complexes are (η^2-1,4-PD)$Cr(CO)_4$ and (η^4-1,4-PD)$Cr(CO)_4$. The third isomer is proposed to be ($\eta^{2:CH}$-1,4-PD)$Cr(CO)_4$ (structure IV in Figure 13, where the metal center is bonded to one ethylene group and one methyl hydrogen on the 1,4-pentadiene ligand). This type of bond is often referred to as an "agostic" bond[36] and consists of a 2-electron Cr–H–C bond analogous to those in the ($\eta^{4:CH}$-diene)$Cr(CO)_3$ complexes observed by Kreiter.[13] Clearly there is some range of metal–hydrogen interactions possible in this type of bond going from a localized Cr–H bond (metal hydride complex) to a localized H–C bond (an η^2 complex). Complexes containing these types of M–H–C bonds are proposed as intermediates in alkyl–alkene isomerization reactions[34] and are also reasonable intermediates for the metal hydride (olefin)M–H complexes observed during diene isomerization reactions involving coordinatively unsaturated organometallics.[19] Alternatively, it might be suggested that reaction 8 merely involves the isomerization between two (η^2-1,4-PD)$Cr(CO)_4$ species (e.g., a conversion between structures where the open site is either cis or trans to the PD ligand) and that ($\eta^{2:CH}$-1,4-PD)$Cr(CO)_4$ is not involved in the mechanism in Scheme V. However, as seen from this scheme, this assertion would be inconsistent with the results for the 1,3-PD system since the product of reaction 6d would then be (η^4-1,4-PD)$Cr(CO)_4$. If so, the saturated η^4-complex would be preferentially formed at *low* buffer gas pressures (reaction 6d), while the unsaturated η^2 species would be preferred at *high* buffer gas pressures (reaction 6r). It would be surprising if the conjugation of the incoming diene ligand caused this drastic contrast with the 1,3-PD mechanism (where added buffer gas *enhances* the formation of (η^4-PD)$Cr(CO)_4$ at the expense of the η^2-complex as seen in Scheme III). Additionally, the spectrum for (η^4-1,4-PD)$Cr(CO)_4$ (if it were species A, the product of reaction 6d) would resemble that for (η^2-1,3-PD)$Cr(CO)_4$ more closely than that for (η^4-1,3-PD)$Cr(CO)_4$ (compare Figures 2 and 11). From these considerations, we conclude (1) that (η^4-1,4-PD)$Cr(CO)_4$ is not a product of reaction 6d, the dominant channel at low buffer gas pressures, (2) that therefore reaction 8, the conversion of B to C, does not merely involve the isomerization between two (η^2-1,4-PD)$Cr(CO)_4$ complexes but that actual bond-making or -breaking for the η^4-species occurs during this step, and finally, (3) that the bonding of the third species involved in the mechanism in Scheme V is distinct from that of the η^2- and η^4-complexes and is most likely the ($\eta^{2:CH}$-1,4-PD)$Cr(CO)_4$ complex.

Scheme VI

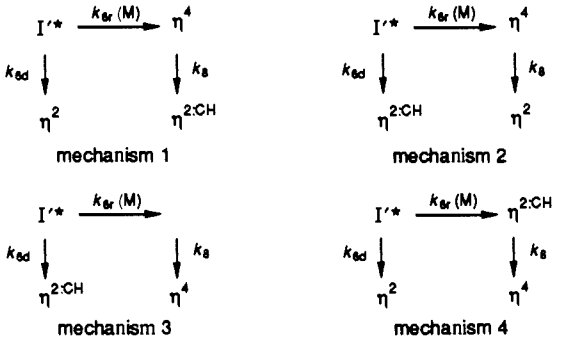

Scheme VI illustrates the four remaining possible reaction mechanisms obtained by assigning each of the possible (1,4-PD)$Cr(CO)_4$ complexes in Figure 13 to species *A*, *B*, and *C* in Scheme V. For simplicity, reaction 7, the relaxation of *A** to *A*, has not been included. The major features of each mechanism will now be discussed in an effort to determine the specific mechanism most likely to explain the reactions of 1,4-pentadiene with $Cr(CO)_4$.

Mechanism 1 implies that I'* is [(η^4-1,4-PD)$Cr(CO)_4$]*. This species can form (η^2-1,4-PD)$Cr(CO)_4$ by breaking one of its Cr–ethylene bonds or form (η^4-1,4-PD)$Cr(CO)_4$ by collisional relaxation. Upon forming (η^4-1,4-PD)$Cr(CO)_4$, the strain induced by having the ethylene groups in (η^4-1,4-PD)$Cr(CO)_4$ separated by an additional C–C bond relative to the stable (η^4-1,3-PD)$Cr(CO)_4$ complex is relieved by replacing one of the Cr–ethylene bonds with a Cr–H–C bond (compare structures I, II, and IV in Figure 13). This "freeing up" of an ethylene bond in step 8 seems consistent with the magnitude of the pre-exponential factor for k_8 ($\sim 10^{13}$ s^{-1}). The pre-exponential factor for the loss of C_2H_4 from $(C_2H_4)_2Fe(CO)_3$ (10^{17} s^{-1}) is somewhat larger than this,[26] as would be expected for the *complete* loss of a ligand. It is likely that the analogous rearrangement and resulting agostic M–H–C bond in step 8 is not observed in the 1,3-pentadiene system because of the stability of (η^4-1,3-PD)$Cr(CO)_4$.

Mechanism 2 is similar to mechanism 1 except that the assignments for (η^2-1,4-PD)$Cr(CO)_4$ and ($\eta^{2:CH}$-1,4-PD)$Cr(CO)_4$ have been switched. In this mechanism, the assignment for I'* becomes ambiguous; it is either [(η^4-1,4-PD)$Cr(CO)_4$]* or [($\eta^{2:CH}$-PD)$Cr(CO)_4$]*. The major reason to prefer mechanism 1 to 2 is that the relaxation of I'*, reaction 6d, can proceed more efficiently through bond scission than through a rearrangement of the Cr/1,4-PD bonds.

Mechanism 3 appears less likely than mechanism 1 or 2. Reaction 8 is activated and has a large pre-exponential factor. If reaction 8 involved the addition of the second ethylene bond to (η^2-1,4-PD)$Cr(CO)_4$, it is reasonable to expect that the rate constant for this process would have a negligible activation energy and a low pre-exponential factor, as observed for the formation

of $(\eta^4$-1,3-PD)$Cr(CO)_4$ from $(\eta^2$-1,3-PD)$Cr(CO)_4$ in section III.B.4.

Mechanism 4 is similar to mechanism 1, except that the most reasonable structure for I'* in mechanism 4 is $[(\eta^{2:CH}$-1,4-PD)-$Cr(CO)_4]$*. Another contrast with mechanism 1 is that reaction 8 would imply the conversion of $(\eta^{2:CH}$-1,4-PD)$Cr(CO)_4$ to the more rigid $(\eta^4$-1,4-PD)$Cr(CO)_4$ complex. The large pre-exponential factor observed for this step makes this assignment unlikely since this type of conversion is expected to be entropically disfavored. Additionally, by comparing structures II and IV with the stable $(\eta^4$-1,3-PD)$Cr(CO)_4$ complex (structure I) in Figure 13, one would expect that $(\eta^{2:CH}$-1,4-PD)$Cr(CO)_4$ is more stable than $(\eta^4$-1,4-PD)$Cr(CO)_4$ and that the reaction to form the latter is unimportant for the following reasons. The bonding ethylene groups in $(\eta^4$-1,3-PD)$Cr(CO)_4$ (structure I in Figure 13) are separated by approximately one C–C bond. By comparison, the bonding units in $(\eta^{2:CH}$-1,4-PD)$Cr(CO)_4$ (structure IV in Figure 13) consist of one ethylene group and one methyl C–H group and are also separated by approximately one C–C bond, while the two bonding ethylene groups in $(\eta^4$-1,4-PD)$Cr(CO)_4$ (structure II in Figure 13) are separated by *two* C–C bond lengths. Molecular models indicate that this increased distance requires either a distortion in the CO ligands or a lengthening of the Cr/1,4-PD bond, which implies that $(\eta^4$-1,4-PD)$Cr(CO)_4$ is less stable than $(\eta^{2:CH}$-1,4-PD)$Cr(CO)_4$.

From these comparisons, it is clear that mechanism 1 presents the most physically reasonable picture of the kinetics governing this system. An attempt was made to definitively assign the $(\eta^2$-1,4-PD)$Cr(CO)_4$ complex by adding CO to the reaction cell with the hope of forming $(\eta^2$-1,4-PD)$Cr(CO)_5$. However, none of the three species that are present following the reaction of $Cr(CO)_4$ with 1,4-PD undergo a secondary reaction with CO on a millisecond time scale. This implies that the open site in $(\eta^2$-1,4-PD)$Cr(CO)_4$ is too hindered or there is too high an activation energy for facile addition of a CO ligand. However, it is important to note that addition of CO *does* occur in the 1,4-pentadiene system on a time scale observable with a conventional FTIR spectrometer. The addition of CO is not observed in the 1,3-pentadiene system under the same experimental conditions. This result certainly reflects the differences in the kinetics governing these systems. While the η^2-complex in the 1,3-pentadiene system converts to the η^4-complex on a millisecond time scale, the η^2 and agostic M–H–C bonded complexes in the 1,4-pentadiene system do not form a stable η^4-complex but are stable long enough for one or both species to add CO to form $(\eta^2$-1,4-PD)$Cr(CO)_5$.

Further experimental confirmation of mechanism 1 could perhaps be obtained by a study of the reaction of $Cr(CO)_4$ with other ligands such as butadiene, which does not contain a methyl group and, therefore, would not be expected to form an "agostic" Cr–H–C bond. Another possible ligand is cyclooctadiene, whose methyl groups are not in a favorable position to form an agostic bond.[12]

D. Overall Mechanism for 1,3- and 1,4-Pentadiene. Scheme VII contains the overall mechanism for the reactions of both 1,3- and 1,4-pentadiene with $Cr(CO)_4$. It is not intended that this scheme imply specific geometric information but rather that it indicate mechanistic pathways. Reaction 5 is not observed for 1,4-pentadiene most likely because formation of the resulting rigid, strained, complex (structure II in Figure 13) would imply an even lower pre-exponential factor and greater activation energy than seen in the 1,3-PD systems. Reaction 8 is not observed for 1,3-pentadiene since $(\eta^4$-1,3-PD)$Cr(CO)_4$ is stable.

The mechanisms in Scheme VII imply that addition of pentadiene to $Cr(CO)_4$ and subsequent reactivity of the initially formed complex are *not primarily governed by conjugation of the diene.* It is important to note that this conclusion does not depend on the assignment for species *A*, *B*, and *C* in Scheme V but rather can be drawn solely from a comparison of the short and long time scale behavior in the 1,3- and 1,4-pentadiene systems. For both dienes, the results show the initial formation of an excited complex, which is referred to as $[(\eta^4$-PD)$Cr(CO)_4]$* (sections III.B.4 and III.C.4) and which undergoes a reaction with

Scheme VII

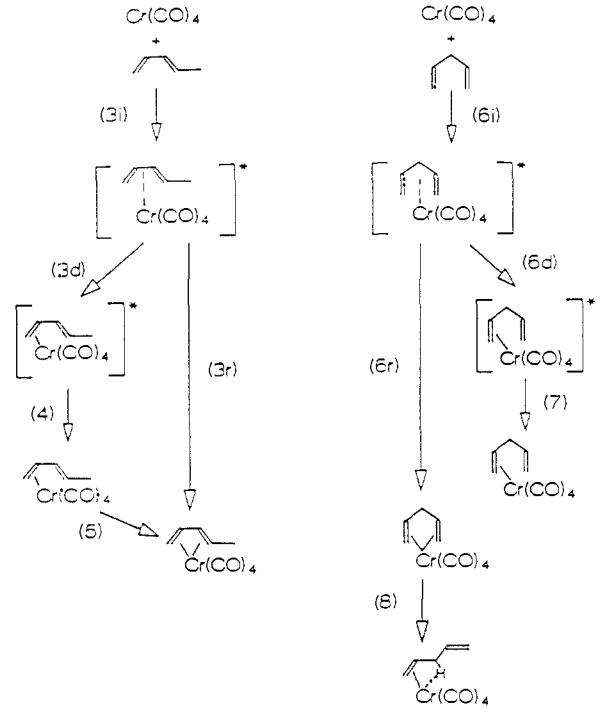

two parallel branches to form $(\eta^2$-PD)$Cr(CO)_4$ and $(\eta^4$-PD)Cr-$(CO)_4$.

The major difference between the reactivities of 1,3- and 1,4-pentadiene is found on longer time scales where the formation of stable $(\eta^4$-1,3-PD)$Cr(CO)_4$ has been observed but that of $(\eta^4$-1,4-PD)$Cr(CO)_4$ is not. In support of the assertion that conjugation is *not* a dominant feature in determining the reaction pathways in these systems, it is useful to consider the following line of reasoning. One would expect that the conjugation of 1,3-pentadiene would affect its reactivity less after it is complexed to $Cr(CO)_4$ than when it is an unbonded molecule. When 1,3-pentadiene is partially bonded to $Cr(CO)_4$ in the $(\eta^2$-1,3-PD)-$Cr(CO)_4$ complex, the degree of conjugation of the π-orbitals of the diene must be reduced since one of these π-orbitals is donating electron density to the metal center. However, it is clear that the reactivities of the η^2-1,3- and η^2-1,4-pentadiene complexes differ quite significantly by comparing the long time scale kinetics in sections III.B.4 and III.C.4. Therefore, it appears that the principal factor that influences the kinetic behavior of these species following the addition of pentadiene to $Cr(CO)_4$ is the relative geometry of the double bonds in the reacting diene, which, in the 1,3-pentadiene case, leads to better overlap of the diene double bonds with the open sites on $Cr(CO)_4$ and formation of a stable $(\eta^4$-PD)$Cr(CO)_4$ complex. Because of the similarities in the short time scale reactivity of $Cr(CO)_4$ with 1,3- and 1,4-pentadiene, it appears that the driving force in the initial reactive steps is due to the electrophilicity of $Cr(CO)_4$ and the electron-donating abilities of the incoming dienes, *not* to the conjugation of these dienes. Conjugated or not, pentadiene ligands rapidly form complexes with $Cr(CO)_4$.

It is interesting to note that the yield of the η^4-products in the reaction of $Cr(CO)_4$ with both 1,3- and 1,4-pentadiene is dependent on the buffer gas pressure (collision frequency), while the yields and rates of simple addition reactions of small monodentate ligands to coordinatively unsaturated metal carbonyls are often not sensitive to buffer gas pressures in this pressure regime.[21] In the case of the diene reactions, two metal ligand bonds are being formed and the bond energy due to both of the bonds must be distributed among the internal degrees of freedom of the molecule. Thus, the resulting adduct molecule is excited to an energy level that corresponds to the vibrational heat bath energy plus the sum of the bond energies for the two diene–metal bonds. If the two diene–metal bonds have similar bond energies, then the total energy of the adduct is significantly above the critical energy for

breaking one diene–metal bond. In the case of the addition of a monodentate ligand, the entire system will be above the critical energy only by an amount due to the thermal heat bath energy. By using a simple model for unimolecular dissociation,[21b] it is clear that when the two metal–pentadiene bonds have similar bond dissociation energies, the rate constant for dissociation of one of the metal–diene bonds from $[(\eta^4\text{-PD})Cr(CO)_4]^*$ is much larger than the rate constant for dissociation of a simple ligand, such as CO, from $[Cr(CO)_5]^*$ formed by the recombination of CO and $Cr(CO)_4$.

The geometry of the incoming ligand also provides a reasonable explanation for the behavior of other diene systems. From the relative decay rates for $(C_2H_4)_2Cr(CO)_4$ and $(\eta^4\text{-}C_4H_6)Cr(CO)_4$ in Table II,[12,14] it can be seen that the conjugated butadiene complex is more stable. This may be explained by considering that the repulsion of hydrogens on the ethylene ligands in $(C_2H_4)_2Cr(CO)_4$ forces these ligands to be further separated than the ethylene groups in butadiene, which are joined by a C–C bond. On the other hand, as stated previously, Dixon et al.[12] observed that conjugated diene complexes (with, for example, butadiene) were *less* stable than nonconjugated diene complexes (with, for example, cyclooctadiene). From their results, one would expect that the bonding orbitals on Cr overlap the ethylene groups in cyclooctadiene, which are positioned parallel to each other, much better than they overlap the ethylene groups in butadiene, which are tilted at an angle of ~60° relative to each other. From these two comparisons, it appears that, as in our system, the geometry of the diene ligand can be an important factor in determining the reactivity and/or stability of the resulting complex.

IV. Conclusion

With use of time-resolved IR spectroscopy, the mechanism for and the kinetics of the addition of 1,3- and 1,4-pentadiene to $Cr(CO)_4$ in the gas phase have been determined. The addition of 1,3-pentadiene to $Cr(CO)_4$ results in the formation of a highly excited complex, which is referred to as $[(\eta^4\text{-1,3-PD})Cr(CO)_4]^*$. This complex can collisionally relax to form $(\eta^4\text{-1,3-PD})Cr(CO)_4$ or it can relax via bond scission to form $(\eta^2\text{-1,3-PD})Cr(CO)_4$. The $(\eta^2\text{-1,3-PD})Cr(CO)_4$ complex can then rearrange via a longer time scale first-order process to $(\eta^4\text{-1,3-PD})Cr(CO)_4$. FTIR spectroscopy confirms that both pathways result in the generation of the long-lived species, $(\eta^4\text{-1,3-PD})Cr(CO)_4$. By monitoring selected frequencies in the short time scale spectra, the rate constant for the addition of 1,3-pentadiene to $Cr(CO)_4$ is determined to be $[(6 \pm 2) \times 10^{14}$ cm^3 mol^{-1} s$^{-1}]$, which is near the gas kinetic limit. The species resulting from bond scission of $[(\eta^4\text{-1,3-PD})Cr(CO)_4]^*$, $[(\eta^2\text{-1,3-PD})Cr(CO)_4]^*$, is itself internally excited and is collisionally relaxed by pentadiene with a rate constant of $(4.6 \pm 0.7) \times 10^{13}$ cm^3 mol^{-1} s^{-1} that is considerably smaller than the rate constant for the association reaction. Subsequent conversion of η^2- to $(\eta^4\text{-1,3-PD})Cr(CO)_4$ is a first-order process with a rate constant of $(2.2 \pm 0.9) \times 10^3$ s^{-1} and a negligible activation energy. The relatively small rate constant for this unactivated process is most likely attributable to the highly constrained transition state involved in the attachment of the second diene double bond to the metal center.

For 1,4-pentadiene, diene addition to $Cr(CO)_4$ results in the formation of a highly excited complex, analogous to the 1,3-pentadiene system. The rate constant for this addition reaction, $(4 \pm 2) \times 10^{14}$ cm^3 mol^{-1} s^{-1}, is close to that obtained with 1,3-pentadiene and to the gas kinetic limit. As observed in the 1,3-pentadiene system, this initial complex relaxes either collisionally to $(\eta^4\text{-1,4-PD})Cr(CO)_4$ or via bond scission to form $[(\eta^2\text{-1,4-PD})Cr(CO)_4]^*$. This latter species is then collisionally relaxed by 1,4-pentadiene with approximately the same rate constant as measured for the analogous compound in the 1,3-pentadiene system, $(4.6 \pm 0.7) \times 10^{13}$ cm^3 mol^{-1} s^{-1}. Both the η^2-1,3 and $[(\eta^2\text{-1,4-PD})Cr(CO)_4]^*$ complexes are also relaxed by Ar and other buffer gases. In contrast to what is observed for the 1,3-pentadiene mechanism, $(\eta^4\text{-1,4-PD})Cr(CO)_4$ rearranges to a more stable isomer which is most likely the $(\eta^{2:CH}\text{-1,4-PD})Cr(CO)_4$ complex, while the relaxed species, $(\eta^2\text{-1,4-PD})Cr(CO)_4$, undergoes no further reactivity on the time scale of the TRIR apparatus (≤5 ms). However, neither complex is a stable product on the time scale of several seconds. In the presence of a large excess of CO, $(\eta^2\text{-1,4-PD})Cr(CO)_4$ and/or $(\eta^{2:CH}\text{-1,4-PD})Cr(CO)_4$ can add CO to form the stable $(1,4\text{-PD})Cr(CO)_5$ complex. The first-order rate constant for the $(\eta^4\text{-1,4-PD})Cr(CO)_4$ rearrangement reaction is $(45 \pm 13) \times 10^3$ s^{-1} at 298 K with an activation energy of 11.4 ± 0.4 kcal/mol and a pre-exponential factor of $(8^{+8}_{-4}) \times 10^{12}$ s^{-1}. The high pre-exponential factor, relative to the value for the conversion of $(\eta^2\text{-1,3-PD})Cr(CO)_4$ to $(\eta^4\text{-1,3-PD})Cr(CO)_4$, is due to the entropy gain associated with the "freeing-up" of the ethylene bond in $(\eta^4\text{-1,4-PD})Cr(CO)_4$.

The similarity in the short time scale results between the two systems indicates that the formation of the initial diene–$Cr(CO)_4$ complex is driven by the highly electrophilic nature of the bis-unsaturated $Cr(CO)_4$ molecule. The contrast in the long time scale reactivities of the two systems appears to be due principally to the relative abilities of the η^2-complexes to form saturated $(\eta^4\text{-PD})Cr(CO)_4$ complexes. The difference in reactivity of the two systems seems to originate in geometric considerations. The structure of 1,3-pentadiene allows formation of a stable species, while the structure of 1,4-pentadiene does not. These results indicate that the mechanism governing the addition of pentadiene to $Cr(CO)_4$ depends principally on factors other than the conjugation of the incoming ligand.

Acknowledgment. We thank the National Science Foundation for support of this work under Grant No. CHE-88-06020. We also acknowledge support of the donors of the Petroleum Research Fund, administered by the American Chemical Society, under Grant No. 18303-AC6, 3-C. We thank Dr. Lambertus J. van de Burgt for his assistance with a number of initial experiments.